

The Continental-Scale Soil Moisture–Precipitation Feedback in Europe with Parameterized and Explicit Convection

DAVID LEUTWYLER,^{a,b} ADEL IMAMOVIC,^a AND CHRISTOPH SCHÄR^a

^a *Atmospheric and Climate Science, ETH Zürich, Zürich, Switzerland*

^b *Max Planck Institute for Meteorology, Hamburg, Germany*

(Manuscript received 2 June 2020, in final form 16 March 2021)

ABSTRACT: Soil moisture–atmosphere interactions are key elements of the regional climate system. There is a well-founded hope that a more accurate representation of the soil moisture–precipitation feedback would improve the simulation of summer precipitation on daily to seasonal, to climate time scales. However, uncertainties have persistently remained as the simulated feedback is strongly sensitive to the model representation of deep convection. Here we assess the feedback representation using a GPU-accelerated version of the regional climate model COSMO. We simulate and compare the impact of continental-scale springtime soil moisture anomalies on summer precipitation at convection-resolving (2.2 km) and convection-parameterizing resolution (12 km). We conduct reanalysis-driven simulations of 10 summer seasons (1999–2008) in continental Europe. While both simulations qualitatively agree on a positive sign of soil moisture–induced precipitation, they strongly differ in precipitation frequency: when convection is parameterized, wetter soil predominantly leads to more frequent precipitation events, and when convection is treated explicitly, they primarily become more intense. The results indicate that the sensitivity to soil moisture is stronger with parameterized convection, suggesting that the land surface–atmosphere coupling may be overestimated. In addition, the feedback’s sensitivity in complex terrain is assessed for soil perturbations of different horizontal scales. The convection-resolving simulations confirm a negative feedback for subcontinental soil moisture anomalies, which manifests itself in a local decrease of wet-hour frequency. However, the intensity feedback reinforces precipitation events at the same time (positive feedback). The two processes are represented differently in simulations with explicit and parameterized convection, explaining much of the difference between the two simulations.

KEYWORDS: Atmosphere–land interaction; Climate models; Cloud resolving models; Interannual variability; Seasonal variability

1. Introduction

Soil moisture (SM) exerts a control on the partitioning of net surface radiation into latent and sensible heat fluxes, and thus affects atmospheric stability and precipitation on a wide range of spatial and temporal scales. As memory of past rainfall events is carried by SM into the future, it has been portrayed as a promising candidate for improving subseasonal to seasonal precipitation forecasts (Koster et al. 2000; Dirmeyer 2000; Koster and Suarez 2001). Especially precipitation originating from diurnal convection (thunderstorms and rain showers) can be strongly controlled by SM variability. Although progress in understanding the involved processes has been achieved by virtue of observations and numerical simulations, it remains uncertain when and where to expect positive or negative feedbacks (Hohenegger et al. 2009; Seneviratne et al. 2010; Taylor et al. 2012; Santanello et al. 2018). The nature of the

feedback is fundamental: On seasonal time scales, a dry spring anomaly may carry over to the summer season and amplify summer droughts and heat waves, as explored for a number of European heatwaves (e.g., Fischer et al. 2007). On climate change time scales, the sign and strength of the feedback loop is essential as well: A positive feedback would amplify the response of the system to a larger-scale imposed perturbation, while a negative feedback would moderate the response.

Until the late 1990s, the prevalent line of research on the soil moisture–precipitation (SMP) feedback were observation-based assessments of moisture recycling (Brubaker et al. 1993; Eltahir and Bras 1996). At the time, they assessed a hypothesis suggesting that a substantial fraction of precipitation over wet soils originates directly from evapotranspiration within the same region. Later simulation-based studies suggested that the feedback manifests itself by altering the atmospheric stability, precipitation efficiency, boundary layer dynamics, and cloudiness, rather than local moisture recycling (Shukla and Mintz 1982; Schär et al. 1999; Ek and Holtslag 2004). More recently, the scientific discussion mostly revolved around two questions, focusing on the role of the SMP feedback in seasonal predictions and climate projections (Koster et al. 2011; van den Hurk et al. 2012; Lorenz et al. 2016; Moon et al. 2019) and on the control of spatial

 Denotes content that is immediately available upon publication as open access.

 Supplemental information related to this paper is available at the Journals Online website: <https://doi.org/10.1175/JCLI-D-20-0415.s1>.

Corresponding author: David Leutwyler, david.leutwyler@mpimet.mpg.de

DOI: 10.1175/JCLI-D-20-0415.1



This article is licensed under a [Creative Commons Attribution 4.0 license](http://creativecommons.org/licenses/by/4.0/) (<http://creativecommons.org/licenses/by/4.0/>).

SM variability on the initiation of deep convection (Taylor et al. 2011; Guillod et al. 2015).

The first question aims at identifying variations in the feedback sign, strength, or statistical significance, and attribution to synoptic situation, aridity, atmospheric stability, or location (e.g., Findell and Eltahir 2003; Koster et al. 2004; Ferguson et al. 2012; Tuttle and Salvucci 2016). However, distilling causal relationships out of (lagged) correlation analysis has proven difficult (Findell and Eltahir 1997; Salvucci et al. 2002). For the SMP feedback problem, particular challenges arise from the interplay between autocorrelation and seasonal/interannual variability, as well as from interactions of local and remote scales.

Numerical models bear the advantage that the soil state can be externally specified. While many simulations find an increase of precipitation with increasing evapotranspiration (positive feedback; Seneviratne et al. 2013), uncertainties have remained as the models rely on parameterized deep convection and land surface parameterizations. It has been shown repeatedly that such simulations misrepresent the effect of the unresolved mesoscale dynamics on the SMP feedback, and thus statements about the feedback sign and its spatial distribution are not yet considered robust (e.g., Giorgi et al. 1996; Hohenegger et al. 2009; Taylor et al. 2013). These distinctive and differing conclusions drawn from low- and high-resolution models demonstrate an urgent need to better understand the role of the SMP feedback on continental scales.

The second question is related to the role of SM variability in driving quasi-horizontal thermal circulations in response to horizontal variations in surface fluxes (Ookouchi et al. 1984; Segal and Arritt 1992; Avissar and Liu 1996; Hohenegger and Schär 2020). At the transition zones between dry and wet soils, thermal circulations emerge from air density/pressure gradients: Satellite-based observations have found such circulations to explain the systematic occurrence of deep-convective clouds in flat terrain at soil moisture transition zones in the Sahel (Taylor et al. 2011), Europe (Taylor 2015), and other regions of the globe (Guillod et al. 2015). The circulations are related to density currents (Segal and Arritt 1992; Hohenegger and Stevens 2018), and—similar to cold-air pools, mountain–valley circulations or land–sea breezes—they may locally enhance moisture convergence and provide a dynamical forcing for initiating convection. These circulations have been extensively studied using idealized simulations run at model resolutions capable of resolving convection explicitly.

Avissar and Liu (1996) demonstrated that patches of dry soil receive substantial precipitation as compared to the surrounding moist soil (negative feedback). However, once model configurations become more realistic, the involved dynamics are more complex and the characteristics of the feedback obscured: In particular, the environmental flow can shift the sign of the SMP feedback from negative to positive, as convective cells initiated over dry anomalies propagate to wet regions (Froidevaux et al. 2014). Additionally, the presence of relatively shallow orography appears to neutralize the local SMP feedback (Imamovic et al. 2017). Furthermore, large-scale flow can suppress the development of mesoscale circulations and deep convection initiation in a stably stratified atmosphere (Lee et al. 2019). Ultimately, the atmosphere can also decouple

from the surface state such that the sign or magnitude of the underlying processes becomes independent of the heat flux contrasts imposed by SM anomalies (Cioni and Hohenegger 2018). The degree to which each of the identified processes contributes to the feedback is still an open question.

Convection-resolving simulations allow representing convection and thermally driven circulations more realistically (Hohenegger et al. 2009; Sun and Pritchard 2016). While an explicit representation of the involved processes denotes a step-change in our ability to represent the European summer climate, computational constraints have so far hindered extensive simulations over long time scales or continental-scale computational domains. Nevertheless a few exploratory short-term simulations were accomplished: for example, Baur et al. (2018) assessed the impact of chessboard-like SM patterns on a 24-h forecast of summer precipitation over Germany. While they found negative spatial SMP coupling, the domain-mean precipitation was only little affected by SM patchiness and the domain-mean SMP feedback remained slightly positive. Henneberg et al. (2018) ran ensembles of convection-resolving simulations over northern Germany to test the sensitivity of convective precipitation to soil moisture. They found that only for unrealistically large SM modifications, the impact of SM on precipitation was significantly larger than the ensemble spread. In other words, potential impacts of SM might be strongly masked by the chaotic nature of convection. The role of this complication depends upon the time scale considered. Likely chaos often dominates in individual weather events, but on climate time scales it should become smaller.

We aim at further closing the gap between the two perspectives by reassessing the sensitivity of summertime precipitation to continental-scale spring SM perturbations. More specifically, we conduct European-scale regional simulations with parameterized and explicit convection and outline the sensitivities related to the representation of convection. We consider 10 season-long convection-resolving simulations covering Europe with three differing initial SM distributions, and will address the following questions: 1) What feedback sign do simulations with parameterized or explicit convection produce? 2) Does the response in precipitation manifest itself in the character (frequency, intensity, and timing) of convection?

We start by summarizing the employed climate model and the simulation configuration (section 2). Subsequently we describe the performed experiments. In section 3 we present the results: First the sensitivity of diurnal precipitation to continental-scale SM perturbations is compared in simulations with parameterized and explicit convection (section 3a), including a composite that considers weak synoptic forcing conditions (section 3b). Subsequently, we reconcile our results with those of established simulations (Hohenegger et al. 2009) by considering the spatial scale of the introduced SM anomaly (section 3c). Afterward, we assess how the representation of diurnal convection contributes to the identified differences in model behavior (sections 3d–3f). In section 4, we further discuss the results, and finally conclude the study in section 5. In addition, we provide an analysis addressing the sensitivity of direct moisture recycling in convection-parameterizing and convection-resolving simulations in the appendix.

2. Model and simulations

a. Model description

The simulations are performed with the fully compressible nonhydrostatic limited-area weather and climate model COSMO (Consortium for Small-Scale Modeling model, v4.19, Steppeler et al. 2003). The model is based on the thermo-hydrodynamic Euler equations, discretized on a longitude–latitude–height mesh using finite-difference methods. Forward in time integration is attained using a split-explicit three-stage second-order Runge–Kutta time-stepping scheme (Wicker and Skamarock 2002). Subgrid-scale processes include a single-moment bulk cloud-microphysics scheme with five hydrometeor species (Reinhardt and Seifert 2006) and a radiative transfer scheme based on the δ -two-stream approach (Ritter and Geleyn 1992). Furthermore, a turbulent kinetic energy (TKE)-based parameterization is used in the planetary boundary layer (Mellor and Yamada 1982; Raschendorfer 2001). Depending on resolution, convection is parameterized using the Tiedtke (1989) scheme. Shallow convection remains parameterized at both resolutions.

Land surface processes are parameterized with TERRA_ML, a second-generation, multilayer soil model predicting soil water content using a formulation based on the Richardson equation (Heise et al. 2006). TERRA_ML considers evapotranspiration, infiltration, percolation, capillary movement, and runoff, as well as melting and freezing of snow. Soil hydrology is discretized in seven active soil layers that extend to 2.77 m. The soil parameters for its eight soil types include field capacity, air dryness point, pore volume, wilting point, and heat capacity. The surface is described by an interception storage, covering bare soil or vegetation. Plants are described by monthly varying surface fields that specify fractional plant cover, root depth, and leaf area index. At the lowest model level of the soil model a bedrock formulation is specified. In the current implementation soil water is removed by surface runoff, ground runoff, and gravitational drainage.

In our version of TERRA_ML runoff is formulated independently from terrain steepness, and thus, the overall precipitation amount and soil type typically take a dominant role in determining the SM content in the deeper soil. This leads to wet mountain tops and dry valleys and thus may lead to biases in triggering and deepening of convective precipitation in complex terrain (Imamovic et al. 2017). To circumvent these issues, Schlemmer et al. (2018) recently proposed a computationally inexpensive formulation of a groundwater table that includes a dependency on terrain steepness. Unfortunately, we did not have a compatible implementation available at the time when our simulations were conducted.

The presented simulations have become possible due to a new version of COSMO capable of exploiting the capabilities of graphics processing units (GPUs). These accelerators appear to be better suited for weather and climate codes than current multicore processors, mainly because they provide substantial parallelism, higher memory bandwidth, and improved latency hiding (Owens et al. 2008). Our version supports executing the entire time stepping (physics, dynamics, and a number of diagnostics) on GPU accelerators and thus

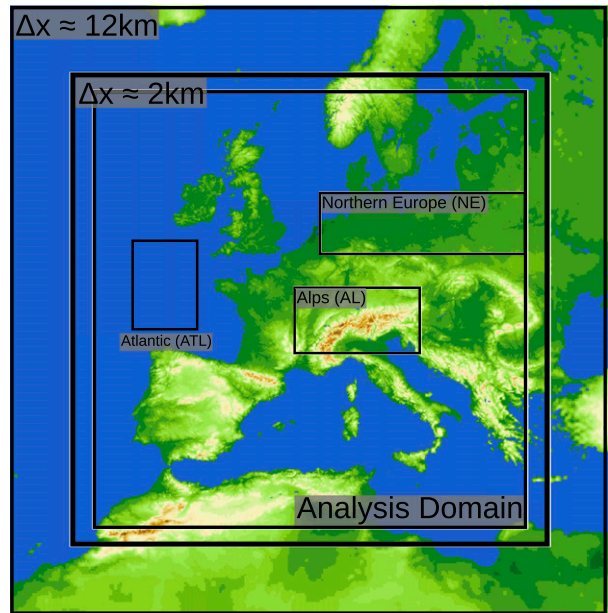


FIG. 1. Integration domains and model topography. The outermost black box denotes the domain of the convection-parameterizing simulation. The bold box denotes the domain of the convection-resolving simulation. The large innermost box indicates the subdomain used in the analysis, and the small boxes (AL, NE, ATL) are subregions used in the recycling model (see the appendix).

avoids expensive data movements between host CPU and GPU accelerators (Führer et al. 2014). In the presented configuration, the new version enables a time compression ratio of about 240 simulation days per day (10 min per simulation day), when the computational domain (see below) is distributed among 144 nodes ($128 \times 128 \times 60$ grid points per node) of the Piz Daint supercomputer (Führer et al. 2018; Schulthess et al. 2019). At the time of writing, this computer is equipped with a single NVIDIA P100 GPU per node.

b. Reanalysis-driven simulations with perturbed soil moisture

The simulations consist of a reference simulation (CTRL; see Leutwyler et al. 2016, 2017) and two simulations with perturbed SM (WET and DRY). They are configured for a computational domain covering most of Europe and follow a two-step one-way nesting approach (Fig. 1). In the outer nest the computational mesh has a horizontal grid spacing of 12 km, employs $355 \times 355 \times 60$ grid points, and uses a parameterization for convection. The inner nest (2 km) has a horizontal grid spacing of 2.2 km, a time step of 20 s, $1536 \times 1536 \times 60$ grid points, and only employs a parameterization for shallow convection. In both simulations, the vertical direction is discretized using 60 stretched model levels ranging from the first model level at 20 m to the model top at 23.5 km. Model analysis is performed on a common domain and excludes grid points close to the boundary relaxation zone. To this end, 240 km of the convection-parameterizing 12-km simulation and 100 km of

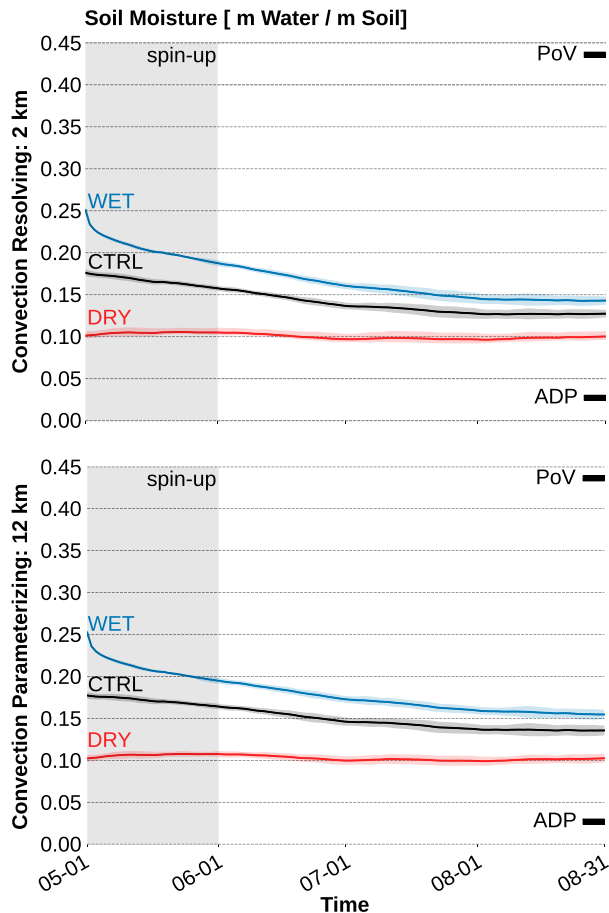


FIG. 2. Evolution of soil moisture in the root zone (upper 1.3 m). Results show averages (solid lines) over the analysis domain in the (top) 12- and (bottom) 2-km simulations. The shading indicates the 10-yr standard deviation. Soil saturation is indicated on right-hand side of each panel in terms of the domain-mean air-dryness point (ADP) and pore volume (PoV). The reference simulation (CTRL) is perturbed for 10 seasons (1999–2008) each initialized 1 May (WET and DRY).

the convection-resolving 2-km simulation are excluded on each side of the domain. The analysis period covers the summer months (JJA) from 1999 to 2008.

The necessary initial and boundary conditions are derived from the European Centre for Medium-Range Weather Forecasts (ECMWF) ERA-Interim reanalysis (Dee et al. 2011). The 12-km simulation was initialized on 1 November 1993 with the soil state from the CCLM EURO-CORDEX simulation of Kotlarski et al. (2014). The 2-km simulation is initialized on 1 November 1998 with the soil state of the 12-km run. Afterward, both CTRL simulations were integrated continuously until 31 December 2008.

Validation of the 10-yr-long CTRL simulation is provided in a number of previous publications. Leutwyler et al. (2017) provided European-scale validation of 2-m temperature, interannual variability of 2-m temperature, surface precipitation, and surface solar radiation. In addition, validation was provided

against hourly rain gauge precipitation datasets where available (Germany and Switzerland), in particular for wet-hour frequency and intensity (99th all-hour percentile; see their Figs. 10–12). Substantial improvements are found for the 2-km simulation in terms of the diurnal cycles of precipitation, despite a weak underestimation of wet-hour frequency over flat terrain. More recently, Hentgen et al. (2019) provided validation of cloud cover fraction and TOA shortwave and longwave radiation fluxes, showing that biases in mean summertime cloudiness and top-of-the-atmosphere radiation budgets are reduced when convection is resolved instead of parameterized. For selected periods (July 2006) and a model setup on an Alpine-scale domain, validation of precipitation and its diurnal cycle is also provided in Heim et al. (2020). The latter study also includes an intercomparison across a range of model grid spacings (from 4.4 to 1.1 km) and an assessment of the role of the model topography’s resolution.

To assess the sensitivity of European summer precipitation to springtime soil moisture, we resimulate the period 1 May–1 September of each year (1999–2008) with initial soil conditions drier or wetter than in CTRL. The modified soil moisture conditions have been obtained by uniformly perturbing the effective soil moisture saturation

$$\Theta = \frac{\theta - \theta_{ADP}}{\theta_{PoV} - \theta_{ADP}} \quad (1)$$

in both nests on 1 May in each layer. Here θ is the volumetric soil water content, θ_{ADP} the air dryness point, and θ_{PoV} the pore volume, as specified for each soil type. The factors applied for the DRY and WET experiments are +25% and –25%, respectively. Note that the 2-km simulations (WET2 and DRY2) are driven by the respective 12-km simulations (i.e., WET12 and DRY12), respectively.

The domain-mean effective soil saturation evolves similarly in both the 12- and 2-km simulations (Fig. 2). In the DRY simulation Θ stays about constant, while CTRL and WET slowly dry out over the course of the summer. The WET simulations rapidly equilibrate toward a new soil water profile while generating substantial runoff. This can be seen by the rapid decrease of SM in WET after the simulation initialization on 1 May. During the 3-month-long analysis period (JJA), the domain-average difference in Θ between WET and DRY decreases, from $\Theta = 15\%$ at the beginning of the simulation to about $\Theta = 8\%$ at the end. The corresponding differences in surface latent and sensible heat fluxes between the WET and DRY simulations, and their diurnal cycles over land, are provided in Figs. S1 and S2 in the online supplemental material.

The multiseasonal simulations are supplemented with month-long sensitivity experiments of July 2006. That period has been assessed before and contains two episodes of consecutive days exhibiting repeated diurnal convection and little disturbances by synoptic weather systems (2–4 July and 11–26 July; see Hohengger et al. 2009; Panosetti et al. 2019; Heim et al. 2020). The simulations (12 and 2 km) were initialized on 1 July 2006, based on the perturbed SM state of the corresponding month from the CTRL simulation. Analysis for the

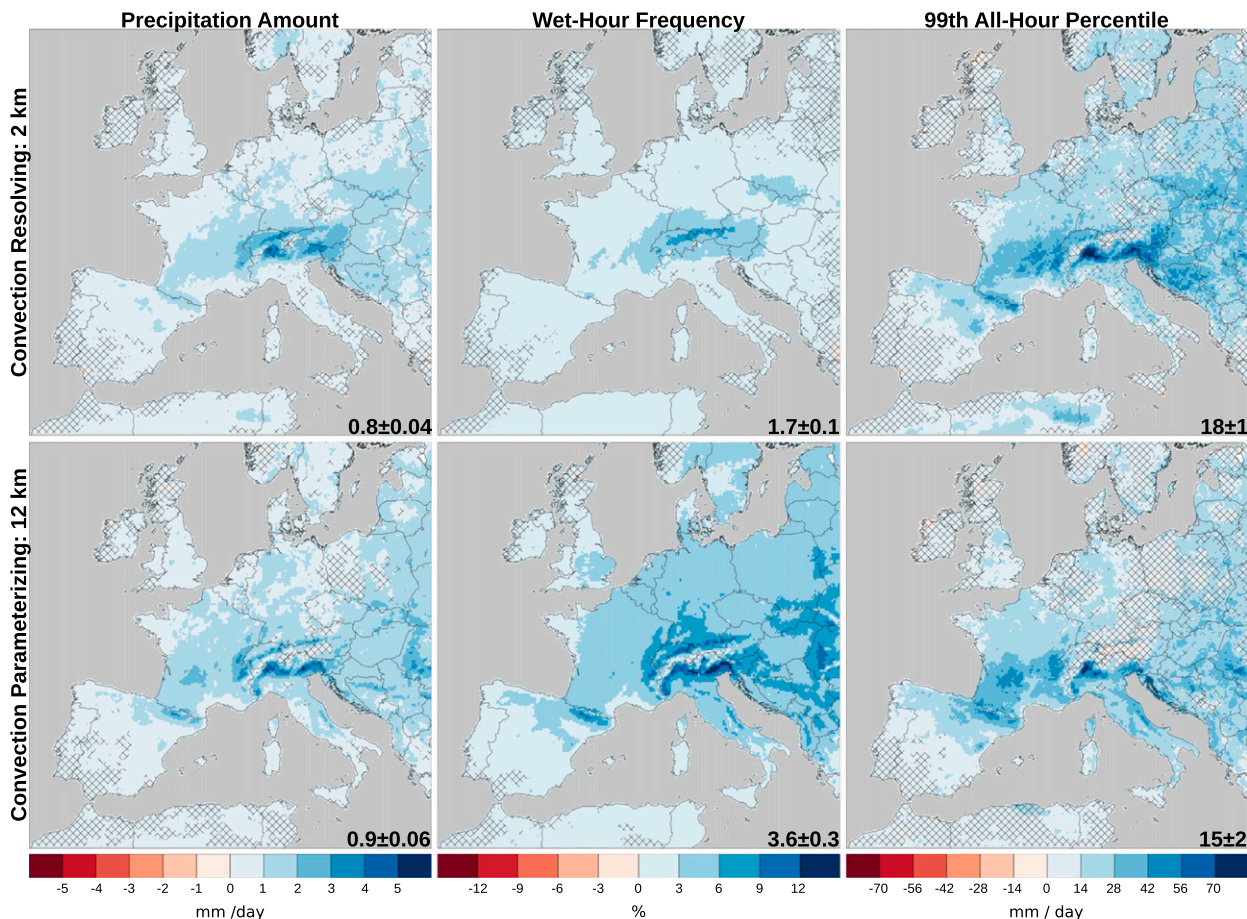


FIG. 3. Absolute differences (JJA mean) between the WET and DRY simulations (colored shading). The hatching marks areas where the difference WET – DRY is small and statistical significance questionable. (left) Precipitation amount, (center) wet-hour frequency, and (right) the all-hour 99th percentile. Positive values (blue) indicate larger precipitation in the WET simulation as compared to DRY. Results are shown for (top) the convection-resolving simulation (2 km) and (bottom) the convection-parameterizing simulation (12 km). The corresponding absolute quantities as derived from CTRL are shown in Fig. S3. Absolute domain-mean differences (WET – DRY) and the 10-yr standard deviations are indicated in the lower-right corner of each panel.

full simulation period and the aforementioned convective episode will be provided separately.

3. Results

In this section, we present the difference in precipitation between the WET and the DRY simulation ($P_{\text{wet}} - P_{\text{dry}}$) for three indices: amount, wet-hour frequency (defined as hours with more than 0.1 mm of precipitation), and intensity (defined as the 99th all-hour percentile; see Schär et al. 2016). Precipitation in the 2-km simulation was aggregated to the computational mesh of the 12-km simulation, before computing the respective indices (see section 2.5 in Leutwyler et al. 2017).

a. Continental-scale soil moisture–precipitation feedback

The simulations with explicit (2 km) and parameterized (12 km) convection agree in that the seasonal-mean feedback between summer precipitation (JJA) and the continental-scale SM state is positive (Fig. 3, left-hand panels). More specifically, a wetter

continent drives a larger precipitation amount, more frequent precipitation events, and more intense precipitation. While the 2- and 12-km simulations agree in a positive seasonal-mean feedback, the imposed springtime SM perturbation leads to a rather different manifestation of the precipitation response: When convection is parameterized the simulations with a wet spring exhibit more frequent summer precipitation events, while more intense events are produced when convection is explicit. This can be seen in the absolute domain-mean differences between WET and DRY, indicated in the lower-right corner of each panel in Fig. 3. The same result can be found when considering relative differences, or in other words, after normalizing the change by the respective index obtained from the CTRL simulation (Table 1, upper rows). The most pronounced distinction between the 12-km and the 2-km simulation can be found for wet-hour frequency. For this index, the 2-km simulation is much less guided by SM than the 12-km one; more specifically, it is only about half as sensitive when considering the relative difference between WET and DRY. In Fig. 3, lack of statistical significance is indicated by the cross-hatching (drawn

TABLE 1. Domain-mean relative percentage difference in precipitation indices over land between WET and DRY simulations, normalized by the CTRL simulations ($(\overline{WET} - \overline{DRY})/\overline{CTRL}$). Note that the indices were first averaged in order to avoid extreme relative differences at grid points where the respective index in CTRL is very small. This occurs for some grid points on the Iberian Peninsula that barely accumulated precipitation. Results are shown for precipitation amount (P), wet-hour frequency (w-h freq.), and the all-hour 99th percentile (p99). In the upper rows indices are shown for averages considering all days of the summer months (JJA) and in the bottom rows for averages only considering conditions of weak synoptic forcing (WSF).

Simulation	P	w-h freq.	p99
12 km	49.6 ± 8.1	45.6 ± 7.3	39.3 ± 9.0
2 km	41.0 ± 4.1	23.5 ± 2.1	39.9 ± 4.3
12 km WSF	73.8 ± 13.8	73.9 ± 12.6	68.1 ± 16.2
2 km WSF	52.6 ± 9.1	28.9 ± 6.4	52.2 ± 9.0

when the change is smaller than the standard deviation of CTRL seasonal means). For large fractions of the domain, the changes in WET – DRY are significant.

Overall, the absolute and relative differences between WET and DRY are most pronounced in the Alpine region. Note that here differences in sensible and latent heat fluxes between WET and DRY are small compared to the remaining domain (see Fig. S1). This indicates that in this region evapotranspiration is not constrained by the availability of soil moisture, but rather by the availability of energy. The surplus of precipitation in WET in comparison to DRY is thus likely a remote effect, driven by

differences in atmospheric humidity stemming from neighboring regions.

The precipitation response is closely linked to the representation of diurnal convection (Fig. 4): In the 12-km simulation, the perturbations imposed on the initial SM state mainly alter the amplitude of precipitation amount and wet-hour frequency and have little effect on the phase of the diurnal cycle. Specifically, the 99th all-hour percentiles of WET and CTRL are very similar. For explicit convection (2 km), the diurnal maxima of amount, frequency, and intensity are systematically delayed by 1–2 h over wetter soils, whereas the onset of precipitation remains at 1000 UTC. Consistent with Fig. 3, a distinct difference in the amplitude of the diurnal cycle can be identified in terms of amount and intensity, while wet-hour frequency is hardly affected by differences in initial SM.

The differences in precipitation intensity can also be identified in the exceedance probability of wet-hour precipitation events (Fig. 5). The metric describes the probability that wet-hour precipitation will exceed a particular threshold. In the 12-km simulation, the distribution is mostly independent of SM: only when the event intensity exceeds 5 mm h^{-1} does the DRY simulation deviate from CTRL, while WET and CTRL hardly differ. In contrast, the 2-km simulation yields overall less intense events for DRY and slightly stronger events for WET.

b. Continental-scale soil moisture–precipitation feedback under weak synoptic forcing

Diurnal convection is common during episodes of weak synoptic forcing (i.e., high or flat pressure) during European summers (e.g., Langhans et al. 2013). To objectively and

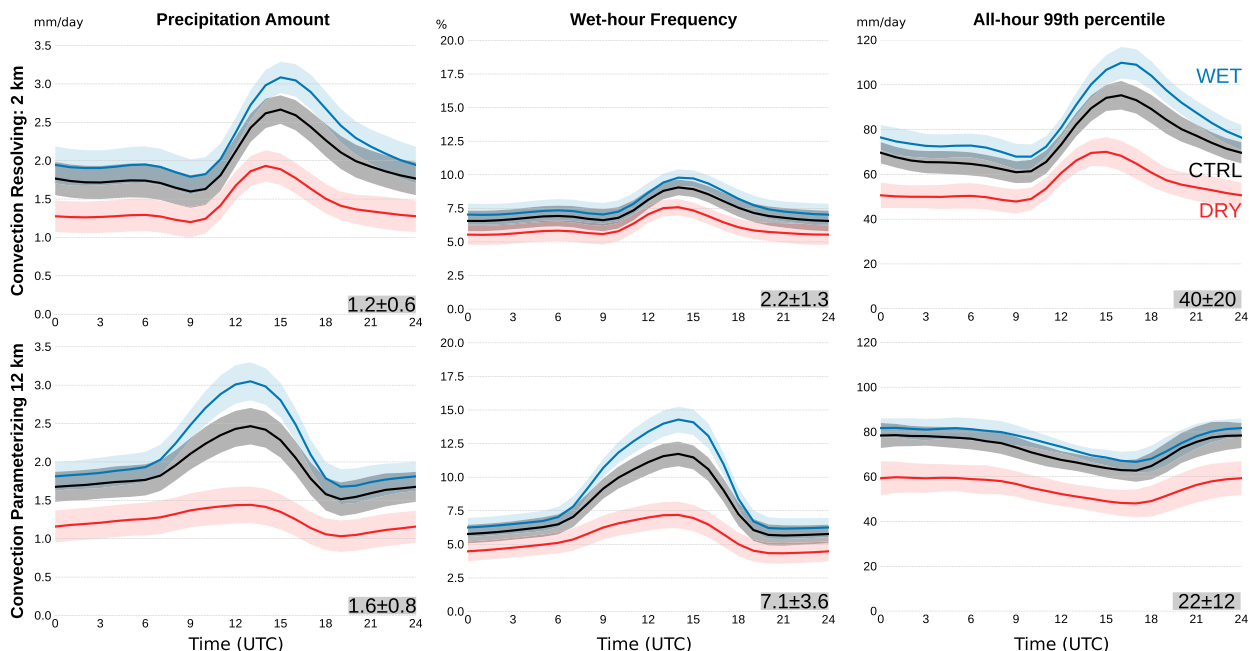


FIG. 4. Seasonal-mean (JJA) diurnal cycles of (left) precipitation amount, (center) wet-hour frequency, and (right) the all-hour 99th percentile. Results are shown for (top) the convection-resolving simulation (2 km) and (bottom) the convection-parameterizing simulation (12 km). The shading indicates the 10-yr standard deviation. The absolute differences of the diurnal maxima between WET and DRY, as well as the corresponding 10-yr standard deviations, are indicated in the lower-right corner of each panel.

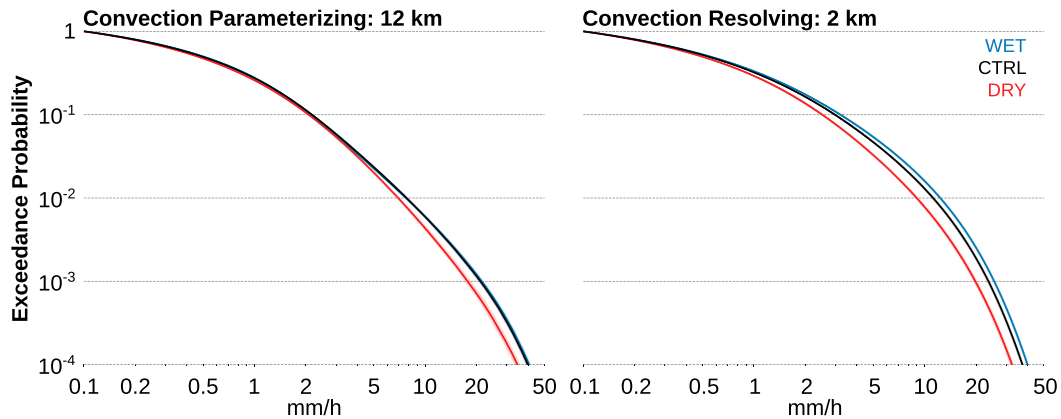


FIG. 5. Cumulative frequency distribution of wet-hour precipitation over land (threshold of exceedance) for the summer season (JJA) in CTRL, WET, and DRY. Analysis is done for (left) the simulation with parameterized convection (12 km) and (right) with explicit convection (2 km). The shading indicates the 10-yr standard deviation. It was obtained by repeatedly (100 times) choosing (with replacement) from the 10 domain-mean distributions at random.

automatically identify such episodes, we use a recently proposed index to filter out summer precipitation related to extratropical cyclones or surface fronts (Rüdisühli et al. 2020). The index is composed of two thresholds applied to geopotential height Z on the 850-hPa pressure level: In the first step extratropical cyclones and the associated frontal systems are removed by disregarding low pressure conditions ($Z > 1450$ m). In the second step, the remaining frontal systems are removed by disregarding areas with strong horizontal pressure gradients ($\nabla_h Z < 0.02 \text{ m m}^{-1}$). To ensure that the filtered model output contains the same number of samples for both models, we apply the method only to the output of the 12-km CTRL simulation and use the same mask to filter the output from the 2-km simulations. As a result, 42% of the hourly model output available over land is discarded. In Scotland or along the west coast of Norway extratropical cyclones are particularly frequent and thus some of the grid points only retain about 14% (3000 hourly samples) of the original model output (21 840 hourly samples).

Without precipitation originating from synoptic systems, the absolute differences in precipitation amount between wet and dry soils are smaller than when the entire model output is considered (Fig. 6). The smaller differences between WET and DRY are due to less precipitation occurring during these conditions. However, when normalizing the indices with the respective index of the CTRL simulation, domain-mean indices become greater under weak synoptic forcing than when all days are considered (Table 1). This confirms that the SMP feedback is stronger during episodes of predominant diurnal convection, but also that the feedback is weaker at 2-km grid spacing. When considering relative (normalized) indices, the difference between WET and DRY is considerably smaller in the 2-km than in the 12-km simulation. This applies to all considered indices, and in particular to wet-hour frequency.

c. Spatial scale of the soil moisture feedback

The results discussed above allow for the interpretation that, on seasonal time scales, the continental-scale SMP feedback is

predominantly positive. However, it is well known that the feedback also exhibits spatial scale dependencies. Applying the SM perturbations on continental scales may thus partly obfuscate negative feedbacks acting at the mesoscale.

Feedbacks at local scales have been suspected to relate to mesoscale circulations driven by spatial SM variability. Here we assess their relevance in complex terrain, such as in the Alps. To this end, we provide three supplementary pairs of month-long simulations of July 2006, each consisting of a convection-parameterizing 12-km simulation and a 2-km simulation. The three simulations are distinct in the horizontal extent of the initial SM perturbations. They range from $270 \times 270 \text{ km}^2$ to $650 \times 1100 \text{ km}^2$, and on to the continental scale (the computational domain of the 2-km simulation). The anomaly is based on the SM state of the respective CTRL simulation on 1 July. For consistency, the 2-km simulations were driven by boundary conditions obtained from a 12-km run without a SM perturbation applied. That is in contrast to the 10-season-long simulation used above, where the nested 2-km simulation is driven by boundary conditions obtained from a 12-km simulation with perturbed SM.

Placing a $270 \times 270 \text{ km}^2$ patch of perturbed SM in the western Alps (WAL) of the 2-km simulation yields a mostly negative feedback coinciding with the spatial scale of the perturbation (green rectangle in Fig. 7, top left-hand panel). When the patch exceeds the scale of the Alps (AL), it becomes positive along the slopes of the Alpine ridge but remains weakly negative otherwise (Fig. 7, top-center panel). Along the edge of the anomaly a distinct dipole pattern forms, displaying a very weak negative feedback ($< 1 \text{ mm day}^{-1}$) over the perturbed soil and a positive feedback right outside the green rectangle (up to 3 mm day^{-1} ; see Fig. 7, center panel). Once the SM perturbation covers a continental-scale area (EU), the feedback again becomes mostly positive (Fig. 7, right-hand panel). Meanwhile, the driving 12-km simulation exhibits a consistently positive feedback in all configurations and typically more precipitation over the plains of France and

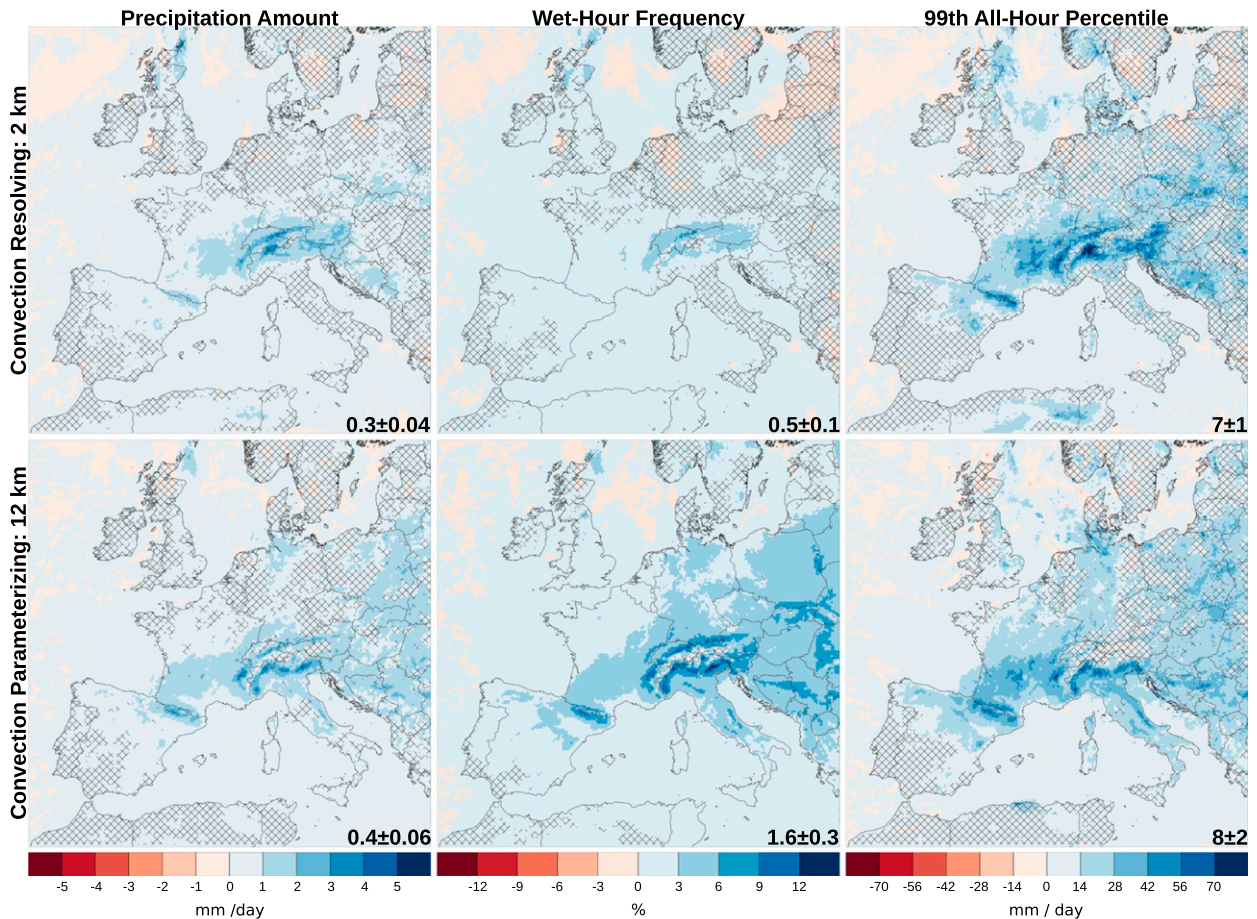


FIG. 6. As in Fig. 3, but for the subset of hours with weak synoptic forcing (see text for details). The corresponding absolute quantities as derived from CTRL are shown in Fig. S4.

Germany (Fig. 7, bottom panels). Consistent with the analysis presented in section 3b, the soil moisture precipitation feedback becomes more positive when considering the entire simulated period (July 2006) rather than only the convective days (2–4 and 11–26 July 2006; see Fig. S5).

d. Vertical profiles and indices of instability

In this section we provide an analysis of convective available potential energy (CAPE) and convective inhibition (CIN) obtained from the month-long EU simulations previously shown in Fig. 7 (right-hand panels). While the short integration period of this simulation limits the robustness of the results, it still appears insightful as both simulations analyzed here yield positive soil moisture–precipitation feedbacks during the convective days analyzed (2–4 and 11–26 July 2006; see Fig. 7, right-hand panels), similar to the full 10-yr simulation (Figs. 3 and 6).

The vertical profiles in Fig. 8 were obtained for one grid point located near the town of Payerne (46.81°N, 6.94°E) in Switzerland (green star in Fig. 7, right-hand panels). It is located on flat terrain between the Jura mountains and the Alps at 456 m above sea level, and has been chosen due to the

pronounced feedback diagnosed in the Alpine region (see Fig. 3). In addition, it resides well outside of narrow mountain valleys, which would hamper direct comparison of results obtained from the two simulations due to the different representations of topography at 2- and 12-km grid spacing.

The analysis shows that surface temperatures in the 2-km and the 12-km simulation are similar, except for a 2-K warmer temperature T in the WET 2-km simulation. That difference in surface temperature is consistent with the slightly less saturated soil, as compared to the 12-km simulation (Fig. 2). Differences in the vertical temperature profiles are restricted to the troposphere (Fig. 8, upper panels). This can be expected since above 11-km height all simulations are relaxed toward the driving data from ERA-Interim. Overall, the 2-km simulation yields a moister midtroposphere (e.g., $T_{d,2\text{km}} - T_{d,12\text{km}} \approx 8 \text{ K}$ on the 500-hPa pressure level) and dryer boundary layer, which is consistent with a strengthened vertical mixing of moisture observed in previous studies (see Leutwyler et al. 2016; Hentgen et al. 2019). Compared to the WET simulation, the profiles of DRY yield warmer T and colder T_d values at the surface, a systematically moister midtroposphere (T_d of DRY is larger than that of WET), and a more elevated lifting

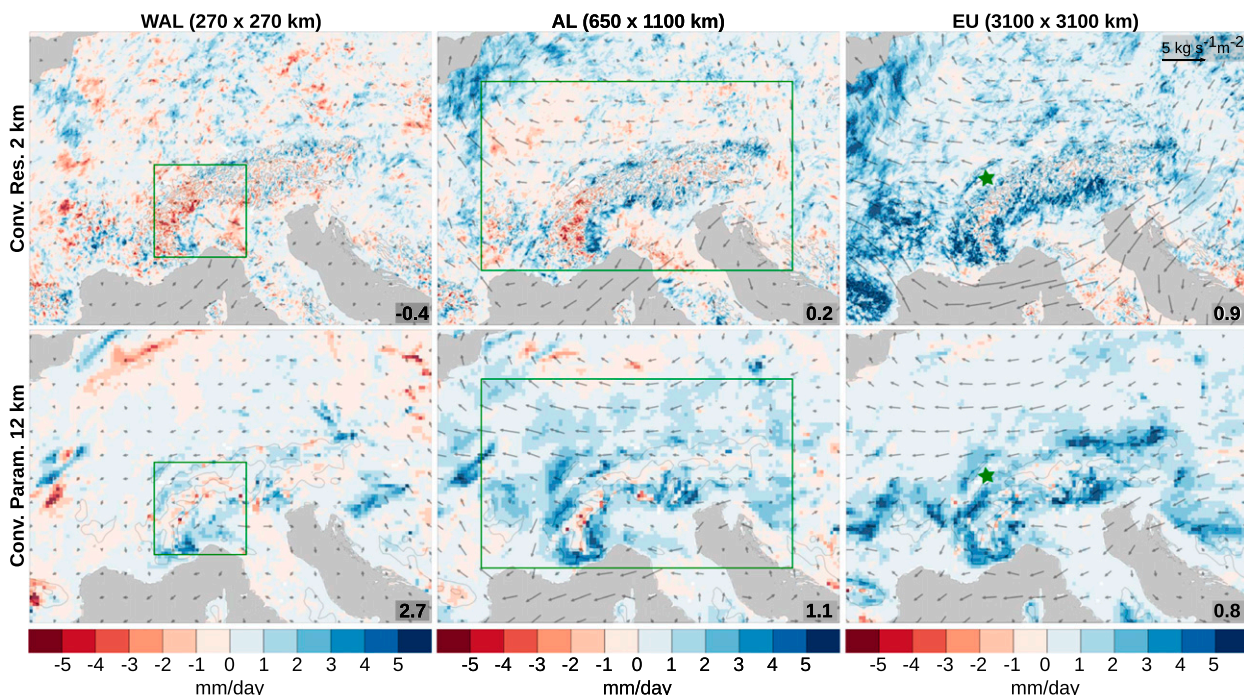


FIG. 7. Zoom into central Europe showing the differences (WET – DRY) in mean rain amount (shading in mm day^{-1}) for three month-long simulation pairs, using soil-moisture perturbations in different subdomains. The initial SM perturbations are applied over (left) the western Alps (WAL; green rectangle), (center) the Alps (AL; green rectangle), and (right) the whole 2-km domain (EU). The results are averaged for an episode of weak synoptic forcing (2–4 and 11–26 Jul 2006). The values in the lower-right corner of each panel indicate absolute differences obtained over the subdomain where the perturbation was applied. The thin gray contours lines show terrain height in steps of 1000 m, and the gray arrows indicate the difference in vertically integrated moisture flux. (top) The simulation with explicit convection (2 km) and (bottom) the simulation with parameterized deep convection (12 km). The green star in the right-hand side panels denotes the location of the vertical profiles shown in Fig. 8. The corresponding figure obtained when considering the entire simulation period (July 2006) is shown in Fig. S5, and two further simulation pairs with even smaller local SM perturbations are shown in Fig. S6.

condensation level (indicated by the sharp corner in the parcel ascent).

The displayed profiles of the 2-km simulations coincide with the time of diurnal maximum CAPE (Fig. 8, lower panels). At noon, the WET 2-km simulation exhibits the highest CAPE of all the simulations (810 J kg^{-1}), while its DRY counterpart exhibits the least (280 J kg^{-1}). At 12-km grid spacing, the diurnal maximum CAPE is reached in the early evening (1900 UTC), and the difference between WET and DRY at 1200 UTC is only about half of that identified at 2-km grid spacing (75 instead of 125 J kg^{-1}).

The disparate diurnal evolution of CAPE in the 12- and 2-km simulations is consistent with the phase shift in the diurnal cycle of precipitation. More specifically, diurnal precipitation in the 2-km simulation peaks in the afternoon (Fig. 4, left-hand panels), and thus the displayed vertical profiles were obtained before the bulk of precipitation occurs. In the 12-km simulation, on the other hand, the precipitation maximum occurs at noon, and thus the displayed vertical profiles were obtained at a time when some of the available CAPE had already been consumed.

Although comparing CAPE and CIN between the 2- and 12-km simulations is difficult, differences in their diurnal evolution appear consistent with the diagnosed differences in the

diurnal cycle of precipitation. At 12-km grid spacing, the WET simulation exhibits more CAPE and more intense precipitation. In addition, it exhibits less CIN during the early morning hours and more frequent precipitation events (higher wet-hour frequency). At 2-km grid spacing, the large difference in CAPE between WET and DRY is consistent with the more intense precipitation obtained in WET (Fig. 4, right-hand panels), and the similar evolution of CIN in WET and DRY is consistent with the small differences in wet-hour frequency.

e. Positive and negative soil moisture feedback for the Alpine-scale soil moisture perturbation

There are pronounced differences in feedback strength depending upon the horizontal scale of the soil moisture perturbations (continental vs Alpine-scale) and the modeling system used (2- vs 12-km simulations), as demonstrated in Fig. 7. What drives the scale and resolution-dependent feedbacks? Our hypothesis is the following: The positive SMP feedback for continental-scale SM anomalies in both the 2- and 12-km simulations result from higher CAPE over wet soils, and thus from more intense precipitation (see section 3d). In contrast, the smaller-amplitude (and sometimes negative) feedback identified in the 2-km simulation with smaller-scale SM perturbations is related to spatial gradients in SM. These

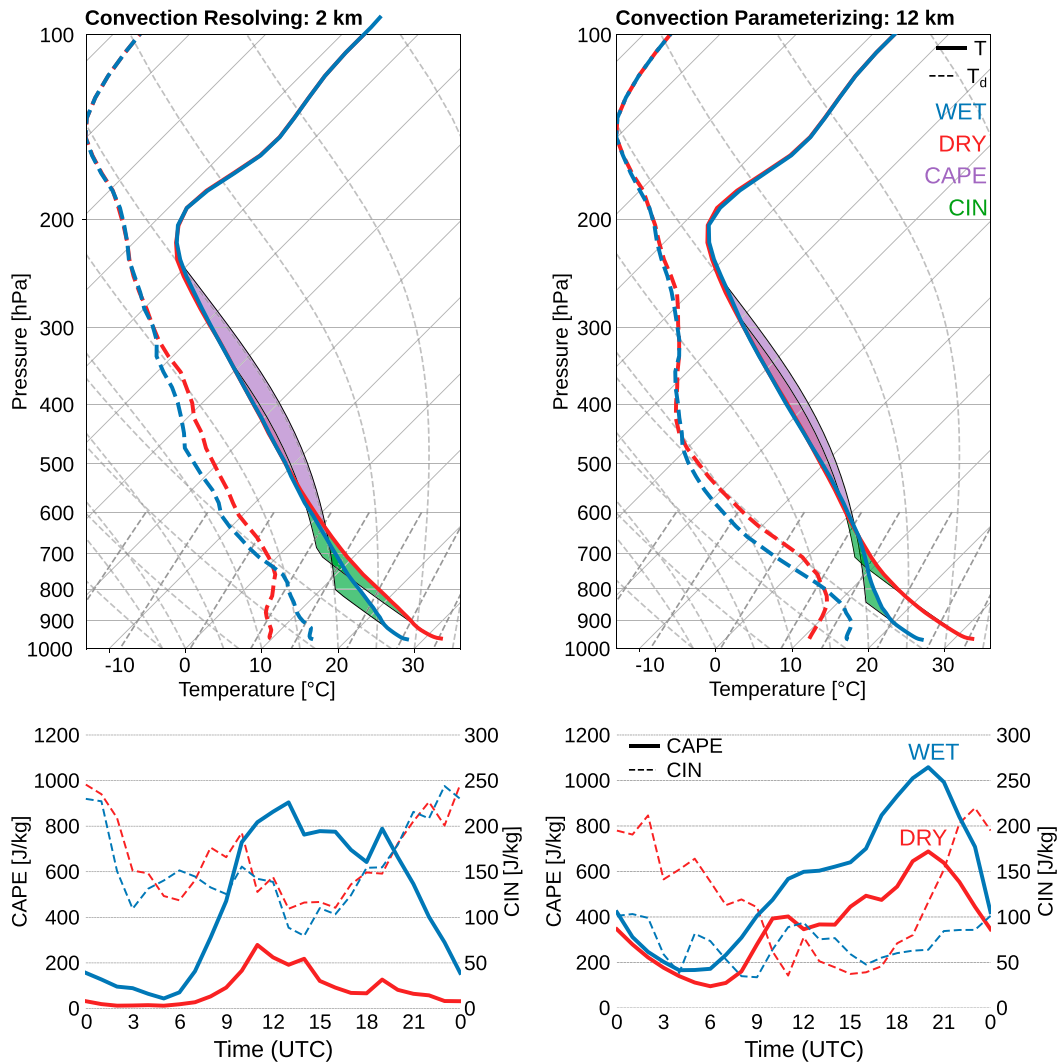


FIG. 8. Convective indices in the month-long EU simulations (Fig. 7, right-hand panels) performed at (left) 2 and (right) 12 km. The indices were averaged for the convective periods 2–4 and 11–26 Jul 2006 and obtained at Payerre (see green star in the right-hand panels in Fig. 7). (top) The skew T - $\log p$ diagrams for the WET (blue) and DRY (red) simulations. The solid lines denote air temperature T and the dashed lines wet bulb temperature T_d at 1200 UTC. The colored shadings denote CAPE (violet) and CIN (green) obtained from an idealized parcel ascent (black line) initialized 50 hPa above the surface. (bottom) Diurnal cycles of CAPE (full lines) and CIN (thin dashed lines). Note that CAPE and CIN are drawn using separate y axes.

gradients drive thermal circulations between wet and dry patches that lead to more frequent triggering and precipitation events over dry soil anomalies, and less frequent events over wet anomalies (see section 1 and the referenced literature). In short, the positive feedback is driven by CAPE and thus precipitation intensity (99th all-hour percentile), while the negative feedback is driven by the triggering process and the associated precipitation frequency (wet-hour frequency). In relation to numerical simulations of the extratropics, CAPE is a central ingredient of convection at any resolution. However, thermally driven circulations and the associated triggering of convection are fundamentally different between explicit and parameterized convection model formulations.

Consistent with the above, the two mechanisms may counteract each other. Below, we aim at illustrating and supporting that hypothesis by, once again, considering wet-hour frequency and intensity separately, but now for the regional SM perturbation discussed in section 3c. For this purpose, we chose the simulation with a SM perturbation applied in the Alpine region (AL; Fig. 7, center panels).

Placing a SM anomaly with spatial extent of $650 \times 1100 \text{ km}^2$ in the 2-km simulation over the Alps results in a negative feedback within the extent of the SM anomaly (green rectangle in Figs. 7 and 9), but nevertheless in a positive mean difference in precipitation amount (0.2 mm day^{-1}). The positive domain mean can be tied to a number of small local patches exerting a

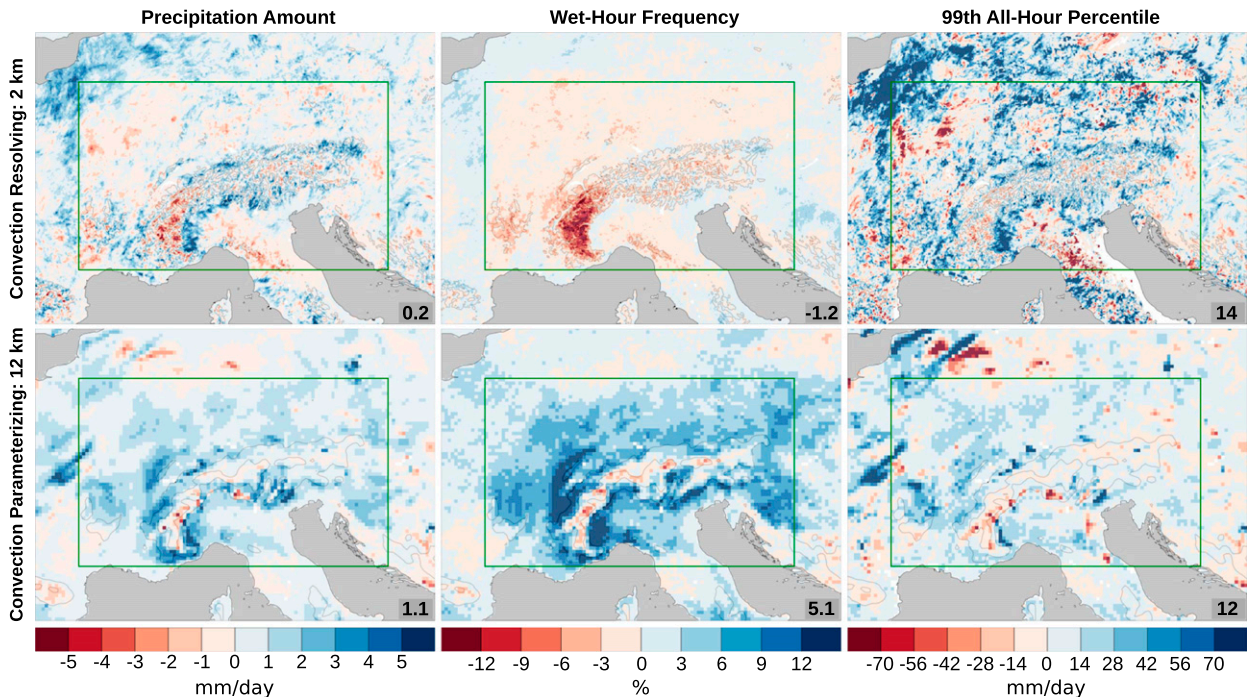


FIG. 9. As in Fig. 3, but for the AL domain presented in Fig. 7. The green rectangle denotes the area where the initial SM perturbation was applied on 1 Jul 2006. The results are averaged for an episode of weak synoptic forcing (2–4 and 11–26 Jul 2006). The values in the lower-right corner of each panel indicate absolute differences between WET and DRY obtained within the area enclosed by the green rectangle.

positive feedback (e.g., along the southern slopes of the Alps) that compensate for the extended areas receiving less precipitation in WET than in DRY.

The spatial distribution of the difference in precipitation amount between WET and DRY is composed of the local wet-hour frequency and precipitation intensity. The difference in wet-hour frequency is negative over a large share of the green rectangle (Fig. 9, top-center panel), and also negative in the domain average (-1.2%). However, at the same time, the difference in precipitation intensity is overall positive ($+14 \text{ mm day}^{-1}$ for the 99th all-hour percentile) and in some locations it exceeds 70 mm day^{-1} (Fig. 9, top-right panel). Ultimately, the two competing mechanisms (frequency and intensity feedbacks) lead to a slightly positive SMP feedback in domain-mean precipitation amount of the 2-km simulation (0.2 mm day^{-1}). In contrast, the three metrics in the 12-km simulation remain mostly positive (Fig. 9, lower panels). The simulations thus lend support to the hypothesis raised in the introductory paragraph of this subsection.

f. Balanced circulation response

In addition to the thermally direct circulations along SM transition zones, differences in soil moisture also lead to a systematic balanced near-surface circulation adjustment (Fig. 10). The circulation anomaly consists of an anticyclonic (cyclonic) circulation in the WET (DRY) simulations, adjusting the pre-existing anticyclonic background circulation. The SM-induced anomaly becomes systematically more

pronounced the larger the SM perturbation is (AL and EU). As a result, the feedback involves differences in the vertically integrated moisture flux ($F_q = \rho q \mathbf{v}_h$; see gray arrows in Fig. 7), consisting of moister near-surface air mass (Δq) and a circulation response ($\Delta \mathbf{v}_h$).

4. Discussion

The strengthening of convection from wet soils in the 2-km simulations is partially consistent with previous theoretical studies. For instance, Froidevaux et al. (2014) found that convective available potential energy (CAPE) is higher over wet soil patches. Higher CAPE enhances the potential for heavy convective events. However, we cannot confirm their results of higher CIN over wetter soil, as CIN in our 2-km simulations did not change between the simulations with continental-scale wet and dry soil perturbations. Likely, that is because in our continental-scale SM anomaly simulation the soil moisture distribution is not so patchy. Furthermore, our results are also consistent with idealized simulations of the SMP feedback of Schlemmer et al. (2012). They found a strong impact of SM on precipitation intensity for a range of atmospheric stability profiles, and a stronger dependency for stable atmospheric conditions. The dependency was attributed to precipitable water being more abundant over wet soils, to reinforced evaporation of precipitation in the relatively dry air over dry soils, and to more CAPE for stable conditions.

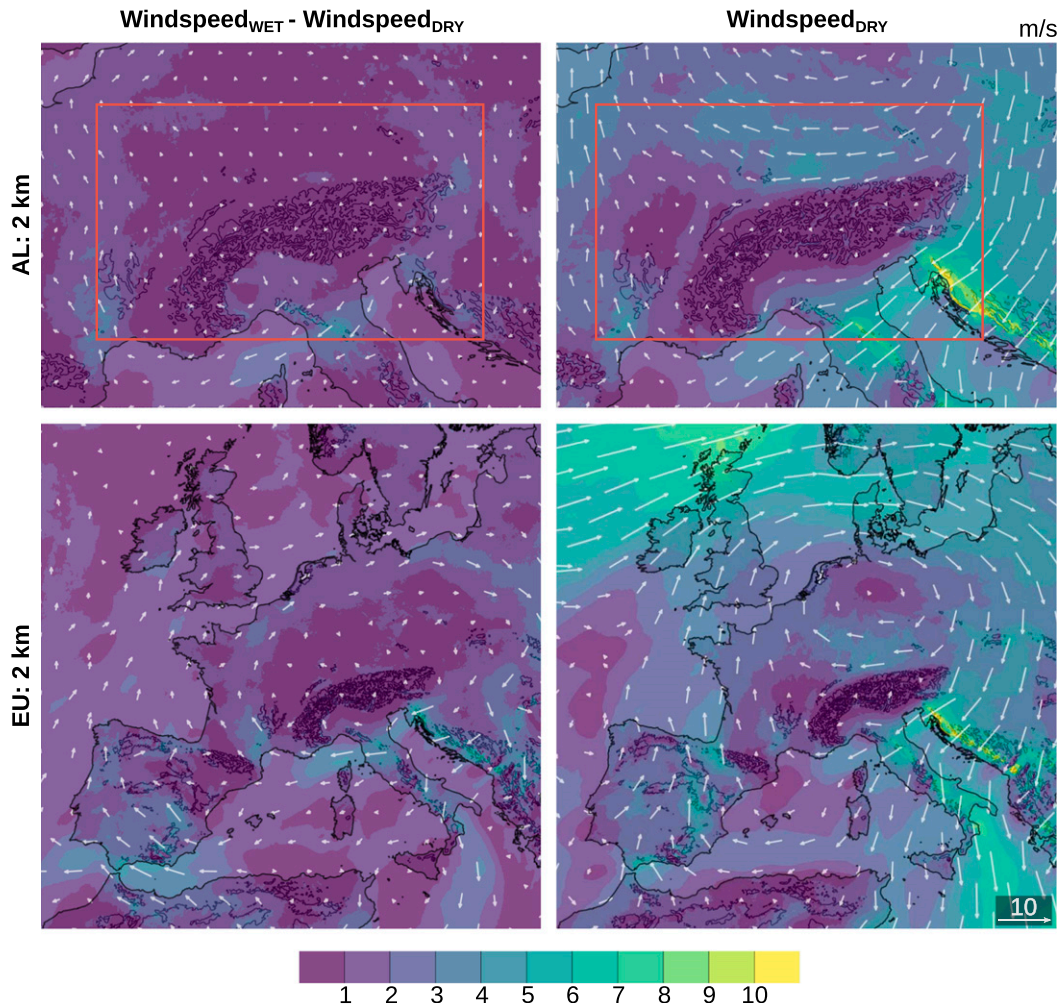


FIG. 10. Horizontal wind at the 850-hPa pressure level in the 2-km simulations, averaged over 2–4 and 11–26 Jul 2006. (left) Averaged differences at between the WET and DRY simulations. The shading and arrows denote the difference in wind speed. (right) Horizontal wind (arrows) and wind speed (shading) in the dry simulation. Zoom into central Europe in a simulation with initial SM perturbations (top) applied over the Alps (AL), and (bottom) applied to the whole 2-km domain (EU). The red rectangle denotes the area with perturbed soil moisture (in the top panels). The corresponding analysis for the 12-km simulation is presented in Fig. S7.

The findings regarding the reduced sensitivity of precipitation frequency, and the enhanced sensitivity of precipitation intensity in the simulations with explicit convection are qualitatively consistent with the study of Sun and Pritchard (2016). Their analysis is based on a simulation employing a superparameterization of convection and on two diagnostics: the triggering feedback strength, a diagnostic assessing the sensitivity of afternoon precipitation frequency on the SM state, and the amplification feedback strength, a joint metric describing the sensitivity of precipitation intensity (see Findell et al. 2015). Employing the superparameterization technique yields substantially reduced triggering feedback strength and slightly enhanced amplification feedback strength, as compared to a simulation with fully parameterized convection. In particular, Sun and Pritchard (2016) also find that changes in wet-hour frequency (triggering feedback strength) in Europe primarily

occur along the Alps (see their Fig. 6a), qualitatively similar to our results.

In the Alps, a strong precipitation feedback occurs despite the small differences in sensible and latent heat fluxes between WET and DRY, both at 2- and 12-km resolution. We suggest that the additional moisture for the increase in precipitation in WET evaporated remotely rather than in the mountain range itself. The Alpine foreland would thus provide the surplus moisture, while local evapotranspiration in the Alps is not overly sensitive to soil moisture effects, consistent with the abundant precipitation and comparatively high soil moisture levels during Alpine summers. In this context it is worth noting that most previous modeling studies of the SMP feedback considered comparatively dry background soil moisture conditions (Avisar and Liu 1996; Froidevaux et al. 2014; Taylor et al. 2013), while here the Alpine region maintains comparatively

moist soil conditions due to orographic precipitation processes. This result is of interest, as it indicates that the consideration of local feedbacks is not showing the whole picture. Over the Alps, there appear to be important remote feedbacks that rely on remote evapotranspiration. The surplus of atmospheric humidity would then reach the Alpine region through large-scale circulations and diurnal circulations. A similar effect might pertain to other European mountain ranges (e.g., the Pyrenees; see Fig. 3), and represent an important element of the SMP feedback in regions of complex topography.

A strong soil moisture intensity feedback seems to suggest a more important role of moisture recycling than previously anticipated. However, a budget analysis following Schär et al. (1999) does not support that hypothesis (see the appendix). With explicit convection, the major contribution to the difference in precipitation amount over selected subdomains still emerges from differences in precipitation efficiency, rather than local evaporation, or from differences in large-scale vertically integrated water fluxes. This suggests that qualitatively bulk recycling does not strongly depend upon parameterized versus explicit convection.

The strong sensitivity of precipitation frequency to SM in our convection-resolving 12-km simulation may relate to the “drizzle problem” of convection parameterizations (e.g., Stephens et al. 2010). In short, the employed Tiedtke (1989) scheme (and others) removes a little piece of instability over a small number of time steps, then switches off for a few steps before switching back on (see, e.g., Keller 2016, Fig. A6 therein). This behavior leads to a substantial and well-known bias in the frequency of light precipitation [see, e.g., Leutwyler et al. (2017) for the 12-km CTRL simulation] and is common for many convection schemes. As a result, the convection scheme will thus remove the additional instability over wetter soils using the same intermittent mechanism, leading to a pronounced sensitivity of precipitation frequency by SM when convection is parameterized.

In the convection-resolving 2-km simulation the overall feedback consists of at least two components: A positive precipitation intensity feedback resulting from higher CAPE over wet soil, and a negative precipitation frequency feedback along gradients in soil moisture. Gradients in soil moisture drive thermal circulations between wet and dry soil leading to more frequent precipitation events over a dry anomaly, and less frequent events over a wet anomaly (e.g., Avissar and Liu 1996; Taylor et al. 2011; Taylor 2015). In practice, the two mechanisms compensate each other, rendering assessments of the feedback sign more complex.

The continental-scale SM anomalies applied in the presented simulations do not necessarily expose the time and length scales of observed anomalies. In fact, even during drought years they often remain on subcontinental scale (see, e.g., Fig. 7 in Naz et al. 2020). Thus the AL simulation (presented in our Fig. 7) may actually portray a closer representation of interannual SM anomalies, although observed anomalies will be smoother, and probably of weaker amplitude. Furthermore, the dependence of the feedback sign on the length scale of the anomaly portrays a challenge when running

climate simulations at convection-resolving resolution, as the underlying land surface models still struggle to correctly represent the spatial and temporal variability of soil moisture (Brocca et al. 2010; Barlage et al. 2015; Furusho-Percot et al. 2019).

On seasonal time scales, the spatial coupling between local SM anomalies and precipitation appears rather weak and scale dependent. This is expected, as a negative feedback reduces soil moisture and surface flux contrasts over time. Nevertheless, it was identified in simulations with complex topography, provided that synoptic forcing is weak. Placing a wet SM anomaly in the western Alps induces a locally negative SMP feedback, which is likely related to stronger plain–valley circulations when the mountains are dry (Imamovic et al. 2017). Consistent with previous studies (Avissar and Liu 1996; Taylor et al. 2012; Taylor 2015), these results suggest that thermally driven circulations may also play a role in the SMPF in complex terrain.

The negative feedback for the Alpine-scale soil moisture perturbation is, in principle, consistent with previous simulations (Hohenegger et al. 2009, see their Fig. 3e). However, the continental-scale computational domain employed in the presented study additionally yields a balanced anticyclonic (cyclonic) circulation response over wet (dry) soils. Such circulation feedbacks have been identified previously for episodes of extreme drought in Europe (Fischer et al. 2007). Thus, differences from the simulation by Hohenegger et al. (2009) may emerge, as the computational domain employed at the time was an order of magnitude smaller (greater Alpine region) than the domain employed in the simulations we conducted. Smaller computational domains typically exert stronger control on the simulation evolution by the lateral boundaries, and thus may suppress a balanced circulation response.

5. Conclusions

We conducted European-scale simulations of 10 summer seasons (May–August) to assess the sensitivity of summer precipitation to springtime soil moisture state in convection-resolving and convection parameterizing simulations. To that end, the continental-scale SM state of a CTRL simulation (Leutwyler et al. 2017) is perturbed every year on 1 May with continental-scale wet and dry perturbations. The soil moisture–precipitation feedback is then assessed based on the precipitation difference emerging from that perturbation.

Averaged over Europe, wetter soils consistently yield more precipitation (positive feedback). The precipitation feedback is particularly pronounced along the slopes of the Alps, despite the small local differences in sensible and latent heat fluxes (section 3a and Fig. S1), suggesting a substantial role for remote moisture supply. While the simulations with parameterized and explicit deep convection agree regarding the sign of the feedback, the difference in domain-mean precipitation between simulations with wet and dry soils is about 20% smaller if convection is resolved explicitly. More importantly, the precipitation coupling evolves in two distinct ways: If convection is parameterized, a wet perturbation primarily

leads to more frequent precipitation events. When treated explicitly, precipitation becomes more intense while the number of precipitation events barely changes, or even decreases when imposing a subcontinental-scale soil moisture anomaly. At the core of the differential SMP coupling in the two simulations lies the representation of diurnal convection. When represented explicitly, a wetter soil yields an amplified diurnal cycle of precipitation intensity and a delayed diurnal precipitation maximum. When convection is parameterized, the timing of the diurnal cycle remains unchanged, and the intensity distribution of diurnal precipitation events is less dependent on SM. Overall, these results suggest that for continental-scale soil moisture anomalies a CAPE-driven soil moisture precipitation intensity feedback is at work, rather than a precipitation frequency feedback. Depending upon the horizontal scale of the soil moisture perturbations (continental vs Alpine-scale) and the modeling system used (2- vs 12-km simulations), the wet-hour frequency feedback can sometimes become negative. In these situations, it moderates the (still positive) intensity feedback.

Considering the results obtained from the presented simulations, our main conclusions are as follows:

- During the European summer, simulations with resolved and parameterized convection yield a positive feedback to continental-scale soil moisture perturbations applied in spring.
- In simulations with resolved convection and a continental-scale springtime soil moisture anomaly, the soil moisture precipitation feedback acts to modulate precipitation amount by intensity, rather than frequency. These differences are fundamental and suggest that for continental-scale SM perturbations a soil moisture intensity feedback should be considered, rather than a precipitation frequency mechanism, or merely a precipitation amount feedback.
- In convection-resolving simulations with subcontinental soil moisture anomalies the feedback in convection-resolving simulations comprises two components: a positive precipitation intensity feedback and a negative wet-hour frequency feedback. In these simulations, precipitation is less sensitive to soil moisture coupling, in particular over flat terrain. Thus, the strength of the soil moisture precipitation feedback may be overestimated in the convection scheme implemented in COSMO (and likely in other models as well).
- The sign and sensitivity of the feedback are sensitive to the spatial scale of the induced soil moisture anomalies. For anomalies with a size exceeding the Alpine scale, a balanced circulation establishes in addition to the direct thermal circulations.

Acknowledgments. We thank Cathy Hohenegger, Linda Schlemmer, and Daniel Regenass for insightful discussions and comments. Also we thank Stefan Rüdüsühli for computing the weak synoptic forcing index for our model output. We would also like to thank Chris Taylor and two anonymous reviewers for their insightful and constructive comments. We acknowledge the Federal Office for Meteorology and Climatology

MeteoSwiss, the Swiss National Supercomputing Centre (CSCS), and ETH Zurich for their contributions to the development of the GPU-accelerated version of COSMO. The Swiss National Science Foundation supported this work under Sinergia Grant CRSII2_154486/1 crCLIM and the Early Postdoc Mobility grant P2EZP2_178503. Finally, we acknowledge PRACE for awarding us compute resources on Piz Daint at the Swiss National Supercomputing Center (CSCS).

Data availability statement. Primary data and scripts used in the analysis and other supplementary information are archived by the Max Planck Institute for Meteorology and can be obtained under the following URL: <http://hdl.handle.net/21.11116/0000-0007-E325-F>. COSMO may be used for operational and for research applications by the members of the COSMO consortium. Moreover, within a license agreement, the COSMO model may be used for operational and research applications by other national (hydro-)meteorological services, universities, and research institutes.

APPENDIX

Reassessing the Recycling Hypothesis

An important question regarding the nature of the SMP feedback relates to the role of locally recycled moisture (Brubaker et al. 1993; Schär et al. 1999). There are two contrasting hypotheses on how evapotranspiration can favor precipitation over wet soils. The direct (i.e., recycling) mechanism relates the surplus of precipitation over wet soils directly to evapotranspiration within the same region (i.e., additional moisture is recycled locally). In contrast, the indirect mechanism suggests that SM feedbacks primarily drive the triggering and deepening of convective cells, while the additional atmospheric moisture input from local evapotranspiration is of minor importance. In that view, moisture is advected from remote sources, and the SMP feedbacks predominantly change precipitation efficiency by altering convection through atmospheric stability and triggering.

The indirect mechanism was supported by simulations with parameterized convection, as they responded to SM with a change in precipitation frequency (i.e., triggering). However, the presented convection-resolving simulations yield more intense precipitation (see section 3) rather than more frequent events (and little change in precipitation frequency). The connection between SM and precipitation intensity suggests that perhaps the “recycling hypothesis” can be supported when convection is resolved explicitly.

a. Water budget and recycling model

Here we test the recycling hypothesis using the output from our convection-resolving simulations. Following Schär et al. (1999), we apply a recycling model, initially developed by Budyko (1974). The method considers the atmospheric water balance, averaged over some time period (say one season) and over some analysis domain (e.g., those shown in Fig. 1). It allows diagnosing the fraction of water evapotranspiring and

TABLE A1. Contributions to the precipitation differences ($\Delta P = \text{WET} - \text{DRY}$; mm day^{-1}) for the three analysis domains presented in Fig. 1. The separation of effects is according to Eq. (A6).

Subdomain	12 km					2 km				
	P_{CTRL}	ΔP	Surface	Remote	Efficiency	P_{CTRL}	ΔP	Surface	Remote	Efficiency
Northern Europe	2.16	1.01	0.01	0.16	0.84	2.18	0.84	0.01	0.15	0.67
Alps	3.13	1.68	0.02	0.15	1.51	3.48	1.65	0.02	0.01	1.62
Atlantic	1.14	0.17	0.00	-0.01	0.18	1.06	0.16	0.00	-0.01	0.17

subsequently precipitating within the same domain (i.e., the recycling rate), as well as the precipitating fraction of the total amount of water entering the domain, either by evapotranspiration or atmospheric transport (precipitation efficiency). In the presented context the recycling model incorporates three assumptions: 1) water vapor derived from within and outside of the analysis domain is well mixed within space and time, 2) precipitation and evapotranspiration have small spatial variability, and 3) lateral flow across the analysis domain is approximately unidirectional (in Europe from west to east). According to the atmospheric water balance, mass conservation of atmospheric water content is

$$\Delta W = \text{IN} - \text{OUT} + \text{ET} - P, \quad (\text{A1})$$

where W is the vertically integrated atmospheric water content, ΔW is its change over a certain time period (say one month or one season), ET is evapotranspiration, and P is precipitation. Moisture convergence ($\text{IN} - \text{OUT}$) of the vertically integrated water flux can be computed from the incoming and outgoing water fluxes (IN and OUT , respectively) using Gauss's theorem. Note that all fluxes are temporally integrated over the time period considered (i.e., one season). The horizontal fluxes need to consider the eddy contributions, and were calculated each model time step on model levels at staggered grid points and using all moist species (see section 2a). The length of the boundary faces were computed at 1/2 the domain height (about 12 km above Earth's surface), accounting for spherical effects (by using the law of Haversines; Korn and Korn 2000).

Assuming uniform moisture recycling within each analysis domain, the bulk recycling ratio β , defined as

$$\beta = \frac{\text{ET}}{\text{IN} + \text{ET}}, \quad (\text{A2})$$

allows quantifying to what extent local evapotranspiration affects precipitable water in the atmospheric column. The joint metric called precipitation efficiency χ diagnoses how much of the available precipitable water is actually precipitating over the domain

$$\chi = \frac{P}{\text{IN} + \text{ET}} \quad (\text{A3})$$

and follows directly from its definition. For the perturbation experiments (see section 2b) Eq. (A3) can be written as

$$P' = \chi'(\text{IN}' + \text{ET}'). \quad (\text{A4})$$

Subtracting (A3) from (A4) and neglecting small nonlinear terms yields

$$\Delta P = P' - P = \underbrace{\chi'(\Delta \text{ET} + \Delta \text{IN})}_{\text{water availability}} + \underbrace{\Delta \chi(\text{ET} + \text{IN})}_{\text{precipitation efficiency}}. \quad (\text{A5})$$

Following the extension by Asharaf et al. (2012), but without making any further approximation, we further split the first term into a surface effect and a remote effect:

$$\Delta P = \underbrace{\chi' \Delta \text{ET}}_{\text{surface effect}} + \underbrace{\chi' \Delta \text{IN}}_{\text{remote effect}} + \underbrace{\Delta \chi(\text{ET} + \text{IN})}_{\text{efficiency effect}}. \quad (\text{A6})$$

The analysis [Eq. (A6)] allows diagnosing the sensitivity of precipitation amount due to differences in evapotranspiration (surface effect), lateral moisture flux (remote effect), and precipitation efficiency (efficiency effect).

An estimate of the errors emerging from the diagnostic approximations can be obtained by comparing the ΔP resulting from Eqs. (A5) and (A6) to the domain mean ΔP_m , as directly obtained from simulation output. Considering each summer of the 10-summer-long perturbation experiment, and each analysis region separately, the imbalance typically amounted to less than a percent. In other words, while the imbalance remains small, the budget relation (A1) is only approximately satisfied. To fully close the budget constraint, we compute the imbalance for each analysis domain

$$\epsilon = \text{IN} - \text{OUT} + \text{ET} - P - \Delta W \quad (\text{A7})$$

and subsequently distribute it equally over the incoming and outgoing lateral water fluxes according to

$$\text{IN}^{\text{corr}} = \text{IN} - \epsilon/2 \quad \text{and} \quad \text{OUT}^{\text{corr}} = \text{OUT} + \epsilon/2. \quad (\text{A8})$$

b. Results

In Table A1 we list the contributions to soil moisture-induced precipitation changes as diagnosed by the recycling model, using three separate subdomains, located in northern Europe, the Alps, and for control over the Atlantic (see Fig. 1). The analysis compares well to the results of Schär et al. (1999), in that the change in precipitation efficiency contributes most to the changes, while remote and surface effects are typically much smaller. According to Schär et al. (1999), this result can be understood when considering that the precipitation efficiency term [$\Delta \chi(\text{ET} + \text{IN})$] contains the vertically integrated flux (IN), which is typically very large. Therefore, a small

change in precipitation efficiency ($\Delta\chi$) will yield a substantial contribution to the overall precipitation change.

The difference in precipitation efficiency ($\Delta\chi$) between the wet and dry simulations combines numerous dynamical and thermodynamical effects [Eq. (A5)], and collects all the processes not explicitly captured by differences in moisture flux across the considered subdomain. Based on the results presented in section 3, we suspect that $\Delta\chi(\text{ET} + \text{IN})$ mainly comprises differences in precipitation intensity and stability, rather than frequency, except for the Alpine region where small differences in precipitation frequency were detected (Fig. 4). However, a more quantitative decomposition still needs to be obtained. For example, an extension of the presented analysis could aim at disentangling the efficiency effect [Eq. (A6)] into remote efficiency ($\Delta\chi_{\text{ET}}$) and surface efficiency ($\Delta\chi_{\text{IN}}$). In other words, what contribution to ΔP can be attributed to the differences in the vertical profile between WET and DRY advected into the analysis domain, and what contribution to the shallower and moister boundary layer over wet soils (see, e.g., Schlemmer et al. 2012). For example, the nonzero results over the Atlantic can be interpreted as a remote efficiency effect, emerging from differences in the atmospheric stability due to more saturated air arriving from the continent.

Overall, the above analysis does not support the recycling hypothesis—consistent with previous studies and irrespective of whether convection is resolved explicitly or parameterized. More specifically, the dominant changes in the domain are due to changes in precipitation efficiency. Nevertheless, it is interesting to note that, for the subdomain located in northern Europe the convection-resolving simulation (2 km) yields a smaller difference in precipitation efficiency (0.67), as compared to the simulation with parameterized convection (0.84). This is consistent with a reduced sensitivity of precipitation to soil moisture.

REFERENCES

- Asharaf, S., A. Dobler, and B. Ahrens, 2012: Soil moisture–precipitation feedback processes in the Indian summer monsoon season. *J. Hydrometeorol.*, **13**, 1461–1474, <https://doi.org/10.1175/JHM-D-12-06.1>.
- Avissar, R., and Y. Liu, 1996: Three-dimensional numerical study of shallow convective clouds and precipitation induced by land surface forcing. *J. Geophys. Res.*, **101**, 7499–7518, <https://doi.org/10.1029/95JD03031>.
- Barlage, M., M. Tewari, F. Chen, G. Miguez-Macho, Z.-L. Yang, and G.-Y. Niu, 2015: The effect of groundwater interaction in North American regional climate simulations with WRF/Noah-MP. *Climatic Change*, **129**, 485–498, <https://doi.org/10.1007/s10584-014-1308-8>.
- Baur, F., C. Keil, and G. C. Craig, 2018: Soil moisture–precipitation coupling over central Europe: Interactions between surface anomalies at different scales and the dynamical implication. *Quart. J. Roy. Meteor. Soc.*, **144**, 2863–2875, <https://doi.org/10.1002/qj.3415>.
- Brocca, L., F. Melone, T. Moramarco, and R. Morbidelli, 2010: Spatial-temporal variability of soil moisture and its estimation across scales. *Water Resour. Res.*, **46**, W02516, <https://doi.org/10.1029/2009WR008016>.
- Brubaker, K. L., D. Entekhabi, and P. S. Eagleson, 1993: Estimation of continental precipitation recycling. *J. Climate*, **6**, 1077–1089, [https://doi.org/10.1175/1520-0442\(1993\)006<1077:EOCPR>2.0.CO;2](https://doi.org/10.1175/1520-0442(1993)006<1077:EOCPR>2.0.CO;2).
- Budyko, M., 1974: *Climate and Life*. International Geophysics Series, Academic Press, 508 pp.
- Cioni, G., and C. Hohenegger, 2018: A simplified model of precipitation enhancement over a heterogeneous surface. *Hydrol. Earth Syst. Sci.*, **22**, 3197–3212, <https://doi.org/10.5194/hess-22-3197-2018>.
- Dee, D. P., and Coauthors, 2011: The ERA-Interim reanalysis: Configuration and performance of the data assimilation system. *Quart. J. Roy. Meteor. Soc.*, **137**, 553–597, <https://doi.org/10.1002/qj.828>.
- Dirmeier, P. A., 2000: Using a global soil wetness dataset to improve seasonal climate simulation. *J. Climate*, **13**, 2900–2922, [https://doi.org/10.1175/1520-0442\(2000\)013<2900:UAGSWD>2.0.CO;2](https://doi.org/10.1175/1520-0442(2000)013<2900:UAGSWD>2.0.CO;2).
- Ek, M. B., and A. A. M. Holtslag, 2004: Influence of soil moisture on boundary layer cloud development. *J. Hydrometeorol.*, **5**, 86–99, [https://doi.org/10.1175/1525-7541\(2004\)005<0086:IOSMOB>2.0.CO;2](https://doi.org/10.1175/1525-7541(2004)005<0086:IOSMOB>2.0.CO;2).
- Eltahir, E. A. B., and R. L. Bras, 1996: Precipitation recycling. *Rev. Geophys.*, **34**, 367–378, <https://doi.org/10.1029/96RG01927>.
- Ferguson, C. R., E. F. Wood, and R. K. Vinukollu, 2012: A global intercomparison of modeled and observed land–atmosphere coupling. *J. Hydrometeorol.*, **13**, 749–784, <https://doi.org/10.1175/JHM-D-11-0119.1>.
- Findell, K. L., and E. A. B. Eltahir, 1997: An analysis of the soil moisture–rainfall feedback, based on direct observations from Illinois. *Water Resour. Res.*, **33**, 725–735, <https://doi.org/10.1029/96WR03756>.
- , and —, 2003: Atmospheric controls on soil moisture boundary layer interactions. Part I: Framework development. *Hydrometeorol.*, **4**, 552–569, [https://doi.org/10.1175/1525-7541\(2003\)004<0552:ACOSML>2.0.CO;2](https://doi.org/10.1175/1525-7541(2003)004<0552:ACOSML>2.0.CO;2).
- , P. Gentine, B. R. Lintner, and B. P. Guillod, 2015: Data length requirements for observational estimates of land–atmosphere coupling strength. *J. Hydrometeorol.*, **16**, 1615–1635, <https://doi.org/10.1175/JHM-D-14-0131.1>.
- Fischer, E. M., S. I. Seneviratne, P. L. Vidale, D. Lüthi, and C. Schär, 2007: Soil moisture–atmosphere interactions during the 2003 European summer heat wave. *J. Climate*, **20**, 5081–5099, <https://doi.org/10.1175/JCLI4288.1>.
- Froidevaux, P., L. Schlemmer, J. Schmidli, W. Langhans, and C. Schär, 2014: Influence of the background wind on the local soil moisture–precipitation feedback. *J. Atmos. Sci.*, **71**, 782–799, <https://doi.org/10.1175/JAS-D-13-0180.1>.
- Fuhrer, O., C. Osuna, X. Lapillonne, T. Gysi, B. Cumming, A. Arteaga, and T. C. Schulthess, 2014: Towards a performance portable, architecture agnostic implementation strategy for weather and climate models. *Supercomput. Front. Innov.*, **1**, 45–62, <https://doi.org/10.14529/JSEFI140103>.
- , and Coauthors, 2018: Near-global climate simulation at 1 km resolution: Establishing a performance baseline on 4888 GPUs with COSMO 5.0. *Geosci. Model Dev.*, **11**, 1665–1681, <https://doi.org/10.5194/gmd-11-1665-2018>.
- Furusho-Percot, C., K. Goergen, C. Hartick, K. Kulkarni, J. Keune, and S. Kollet, 2019: Pan-European groundwater to atmosphere terrestrial systems climatology from a physically consistent simulation. *Sci. Data*, **6**, 320, <https://doi.org/10.1038/s41597-019-0328-7>.
- Giorgi, F., L. O. Mearns, C. Shields, and L. Mayer, 1996: A regional model study of the importance of local versus remote controls

- of the 1988 drought and the 1993 flood over the central United States. *J. Climate*, **9**, 1150–1162, [https://doi.org/10.1175/1520-0442\(1996\)009<1150:ARMSOT>2.0.CO;2](https://doi.org/10.1175/1520-0442(1996)009<1150:ARMSOT>2.0.CO;2).
- Guillod, B. P., B. Orlowsky, D. G. Miralles, A. J. Teuling, and S. I. Seneviratne, 2015: Reconciling spatial and temporal soil moisture effects on afternoon rainfall. *Nat. Commun.*, **6**, 6443, <https://doi.org/10.1038/ncomms7443>.
- Heim, C., D. Panosetti, L. Schlemmer, D. Leuenberger, and C. Schär, 2020: The influence of the resolution of orography on the simulation of orographic moist convection. *Mon. Wea. Rev.*, **148**, 2391–2410, <https://doi.org/10.1175/MWR-D-19-0247.1>.
- Heise, E., B. Ritter, and R. Schrödin, 2006: Operational implementation of the Multilayer Soil Model. Consortium for Small-Scale Modelling (COSMO) Tech. Rep. 9, 20 pp., https://doi.org/10.5676/DWD_pub/nwv/cosmo-tr_9.
- Henneberg, O., F. Ament, and V. Grützun, 2018: Assessing the uncertainty of soil moisture impacts on convective precipitation using a new ensemble approach. *Atmos. Chem. Phys.*, **18**, 6413–6425, <https://doi.org/10.5194/acp-18-6413-2018>.
- Hentgen, L., N. Ban, N. Kröner, D. Leutwyler, and C. Schär, 2019: Clouds in convection-resolving climate simulations over Europe. *J. Geophys. Res. Atmos.*, **124**, 3849–3870, <https://doi.org/10.1029/2018JD030150>.
- Hohenegger, C., and B. Stevens, 2018: The role of the permanent wilting point in controlling the spatial distribution of precipitation. *Proc. Natl. Acad. Sci. USA*, **115**, 5692–5697, <https://doi.org/10.1073/pnas.1718842115>.
- , and C. Schär, 2020: Clouds and land. *Clouds and Climate: Climate Science's Greatest Challenge*, A. Siebesma et al., Eds., Cambridge University Press, 329–355, <https://doi.org/10.1017/9781107447738.013>.
- , P. Brockhaus, C. S. Bretherton, and C. Schär, 2009: The soil moisture–precipitation feedback in simulations with explicit and parameterized convection. *J. Climate*, **22**, 5003–5020, <https://doi.org/10.1175/2009JCLI2604.1>.
- Imamovic, A., L. Schlemmer, and C. Schär, 2017: Collective impacts of orography and soil moisture on the soil moisture–precipitation feedback. *Geophys. Res. Lett.*, **44**, 11 682–11 691, <https://doi.org/10.1002/2017GL075657>.
- Keller, M., 2016: The diurnal cycle of Alpine summer convection in a convection-resolving model: Evaluation with satellite data and sensitivity to atmospheric forcing. Ph.D. dissertation, ETH Zürich, <https://doi.org/10.3929/ethz-a-010658332>, 99 pp.
- Korn, G. A., and T. M. Korn, 2000: *Mathematical Handbook for Scientists and Engineers: Definitions, Theorems, and Formulas for Reference and Review*. McGraw-Hill.
- Koster, R. D., and M. J. Suarez, 2001: Soil moisture memory in climate models. *J. Hydrometeorol.*, **2**, 558–570, [https://doi.org/10.1175/1525-7541\(2001\)002<0558:SMMICM>2.0.CO;2](https://doi.org/10.1175/1525-7541(2001)002<0558:SMMICM>2.0.CO;2).
- , —, and M. Heiser, 2000: Variance and predictability of precipitation at seasonal-to-interannual timescales. *J. Hydrometeorol.*, **1**, 26–46, [https://doi.org/10.1175/1525-7541\(2000\)001<0026:VAPOPA>2.0.CO;2](https://doi.org/10.1175/1525-7541(2000)001<0026:VAPOPA>2.0.CO;2).
- , and Coauthors, 2004: Regions of strong coupling between soil moisture and precipitation. *Science*, **305**, 1138–1140, <https://doi.org/10.1126/science.1100217>.
- , and Coauthors, 2011: The second phase of the global land–atmosphere coupling experiment: Soil moisture contributions to subseasonal forecast skill. *J. Hydrometeorol.*, **12**, 805–822, <https://doi.org/10.1175/2011JHM1365.1>.
- Kotlarski, S., and Coauthors, 2014: Regional climate modeling on European scales: A joint standard evaluation of the EURO-CORDEX RCM ensemble. *Geosci. Model Dev.*, **7**, 1297–1333, <https://doi.org/10.5194/gmd-7-1297-2014>.
- Langhans, W., J. Schmidli, S. Fuhrer, O. Bieri, and C. Schär, 2013: Long-term simulations of thermally driven flows and orographic convection at convection-parameterizing and cloud-resolving resolutions. *J. Appl. Meteor. Climatol.*, **52**, 1490–1510, <https://doi.org/10.1175/JAMC-D-12-0167.1>.
- Lee, J. M., Y. Zhang, and S. A. Klein, 2019: The effect of land surface heterogeneity and background wind on shallow cumulus clouds and the transition to deeper convection. *J. Atmos. Sci.*, **76**, 401–419, <https://doi.org/10.1175/JAS-D-18-0196.1>.
- Leutwyler, D., O. Fuhrer, X. Lapillonne, D. Lüthi, and C. Schär, 2016: Towards European-scale convection-resolving climate simulations with GPUs: A study with COSMO 4.19. *Geosci. Model Dev.*, **9**, 3393–3412, <https://doi.org/10.5194/gmd-9-3393-2016>.
- , D. Lüthi, N. Ban, O. Fuhrer, and C. Schär, 2017: Evaluation of the convection-resolving climate modeling approach on continental scales. *J. Geophys. Res.*, **122**, 5237–5258, <https://doi.org/10.1002/2016JD026013>.
- Lorenz, R., and Coauthors, 2016: Influence of land–atmosphere feedbacks on temperature and precipitation extremes in the GLACE-CMIP5 ensemble. *J. Geophys. Res. Atmos.*, **121**, 607–623, <https://doi.org/10.1002/2015JD024053>.
- Mellor, G., and T. Yamada, 1982: Development of a turbulence closure model for geophysical fluid problems. *Rev. Geophys.*, **20**, 851–875, <https://doi.org/10.1029/RG020i004p00851>.
- Moon, H., B. P. Guillod, L. Gudmundsson, and S. I. Seneviratne, 2019: Soil moisture effects on afternoon precipitation occurrence in current climate models. *Geophys. Res. Lett.*, **46**, 1861–1869, <https://doi.org/10.1029/2018GL080879>.
- Naz, B. S., S. Kollet, H.-J. H. Franssen, C. Montzka, and W. Kurtz, 2020: A 3 km spatially and temporally consistent European daily soil moisture reanalysis from 2000 to 2015. *Sci. Data*, **7**, 111, <https://doi.org/10.1038/s41597-020-0450-6>.
- Ookouchi, Y., M. Segal, R. C. Kessler, and R. A. Pielke, 1984: Evaluation of soil moisture effects on the generation and modification of mesoscale circulations. *Mon. Wea. Rev.*, **112**, 2281–2292, [https://doi.org/10.1175/1520-0493\(1984\)112<2281:EOSMEO>2.0.CO;2](https://doi.org/10.1175/1520-0493(1984)112<2281:EOSMEO>2.0.CO;2).
- Owens, J., M. Houston, D. Luebke, S. Green, J. Stone, and J. Phillips, 2008: GPU computing. *Proc. IEEE*, **96**, 879–899, <https://doi.org/10.1109/JPROC.2008.917757>.
- Panosetti, D., L. Schlemmer, and C. Schär, 2019: Bulk and structural convergence at convection-resolving scales in real-case simulations of summertime moist convection over land. *Quart. J. Roy. Meteor. Soc.*, **145**, 1427–1443, <https://doi.org/10.1002/qj.3502>.
- Raschendorfer, M., 2001: The new turbulence parameterization of LM. *COSMO Newsletter*, No. 1, Consortium for Small-Scale Modeling, Offenbach, Germany, 89–97, http://www.cosmo-model.org/content/model/documentation/newsLetters/newsLetter01/newsLetter_01.pdf.
- Reinhardt, T., and A. Seifert, 2006: A three-category ice-scheme for the LMK. *COSMO Newsletter*, No. 6, Consortium for Small-Scale Modeling, Offenbach, Germany, 115–120, http://www.cosmo-model.org/content/model/documentation/newsLetters/newsLetter06/cnl6_reinhardt.pdf.
- Ritter, B., and J. F. Geleyn, 1992: A comprehensive radiation scheme for numerical weather prediction models with potential applications in climate simulations. *Mon. Wea. Rev.*, **120**, 303–325, [https://doi.org/10.1175/1520-0493\(1992\)120<0303:ACRSFN>2.0.CO;2](https://doi.org/10.1175/1520-0493(1992)120<0303:ACRSFN>2.0.CO;2).

- Rüdisühli, S., M. Sprenger, D. Leutwyler, C. Schär, and H. Wernli, 2020: Attribution of precipitation to cyclones and fronts over Europe in a kilometer-scale regional climate simulation. *Wea. Climate Dyn.*, **1**, 675–699, <https://doi.org/10.5194/wcd-1-675-2020>.
- Salvucci, G. D., J. A. Saleem, and R. Kaufmann, 2002: Investigating soil moisture feedbacks on precipitation with tests of Granger causality. *Adv. Water Resour.*, **25**, 1305–1312, [https://doi.org/10.1016/S0309-1708\(02\)00057-X](https://doi.org/10.1016/S0309-1708(02)00057-X).
- Santanello, J. A., and Coauthors, 2018: Land–atmosphere interactions: The LoCo perspective. *Bull. Amer. Meteor. Soc.*, **99**, 1253–1272, <https://doi.org/10.1175/BAMS-D-17-0001.1>.
- Schär, C., D. Lüthi, U. Beyerle, and E. Heise, 1999: The soil–precipitation feedback: A process study with a regional climate model. *J. Climate*, **12**, 722–741, [https://doi.org/10.1175/1520-0442\(1999\)012<0722:TSPFAP>2.0.CO;2](https://doi.org/10.1175/1520-0442(1999)012<0722:TSPFAP>2.0.CO;2).
- , and Coauthors, 2016: Percentile indices for assessing changes in heavy precipitation events. *Climate Change*, **137**, 201–216, <https://doi.org/10.1007/s10584-016-1669-2>.
- Schlemmer, L., C. Hohenegger, J. Schmidli, and C. Schär, 2012: Diurnal equilibrium convection and land surface–atmosphere interactions in an idealized cloud-resolving model. *Quart. J. Roy. Meteor. Soc.*, **138**, 1526–1539, <https://doi.org/10.1002/qj.1892>.
- , C. Schär, D. Lüthi, and L. Strebel, 2018: A groundwater and runoff formulation for weather and climate models. *J. Adv. Model. Earth Syst.*, **10**, 1809–1832, <https://doi.org/10.1029/2017MS001260>.
- Schulthess, T. C., P. Bauer, N. Wedi, O. Fuhrer, T. Hoefler, and C. Schär, 2019: Reflecting on the goal and baseline for exascale computing: A roadmap based on weather and climate simulations. *Comput. Sci. Eng.*, **21**, 30–41, <https://doi.org/10.1109/MCSE.2018.2888788>.
- Segal, M., and R. Arritt, 1992: Nonclassical mesoscale circulations caused by surface sensible heat-flux gradients. *Bull. Amer. Meteor. Soc.*, **73**, 1593–1604, [https://doi.org/10.1175/1520-0477\(1992\)073<1593:NMCCBS>2.0.CO;2](https://doi.org/10.1175/1520-0477(1992)073<1593:NMCCBS>2.0.CO;2).
- Seneviratne, S. I., T. Corti, E. L. Davin, M. Hirschi, E. B. Jaeger, I. Lehner, B. Orlowsky, and A. J. Teuling, 2010: Investigating soil moisture–climate interactions in a changing climate: A review. *Earth Sci.*, **99**, 125–161, <https://doi.org/10.1016/j.earscirev.2010.02.004>.
- , and Coauthors, 2013: Impact of soil moisture–climate feedbacks on CMIP5 projections: First results from the GLACE-CMIP5 experiment. *Geophys. Res. Lett.*, **40**, 5212–5217, <https://doi.org/10.1002/grl.50956>.
- Shukla, J., and Y. Mintz, 1982: Influence of land-surface evapotranspiration on the earth's climate. *Science*, **215**, 1498–1501, <https://doi.org/10.1126/science.215.4539.1498>.
- Stephens, G. L., and Coauthors, 2010: Dreary state of precipitation in global models. *J. Geophys. Res.*, **115**, D24211, <https://doi.org/10.1029/2010JD014532>.
- Stappeler, J., G. Doms, U. Schättler, H. W. Bitzer, A. Gassmann, U. Damrath, and G. Gregoric, 2003: Meso-gamma scale forecasts using the nonhydrostatic model LM. *Meteor. Atmos. Phys.*, **82**, 75–96, <https://doi.org/10.1007/s00703-001-0592-9>.
- Sun, J., and M. S. Pritchard, 2016: Effects of explicit convection on global land–atmosphere coupling in the superparameterized CAM. *J. Adv. Model. Earth Syst.*, **8**, 1248–1269, <https://doi.org/10.1002/2016MS000689>.
- Taylor, C. M., 2015: Detecting soil moisture impacts on convective initiation in Europe. *Geophys. Res. Lett.*, **42**, 4631–4638, <https://doi.org/10.1002/2015GL064030>.
- , A. Gounou, F. Guichard, P. P. Harris, R. J. Ellis, F. Couvreux, and M. De Kauwe, 2011: Frequency of Sahelian storm initiation enhanced over mesoscale soil-moisture patterns. *Nat. Geosci.*, **4**, 430–433, <https://doi.org/10.1038/NGEO1173>.
- , R. A. M. de Jeu, F. Guichard, P. P. Harris, and W. A. Dorigo, 2012: Afternoon rain more likely over drier soils. *Nature*, **489**, 423–426, <https://doi.org/10.1038/nature11377>.
- , C. E. Birch, D. J. Parker, N. Dixon, F. Guichard, G. Nikulin, and G. M. S. Lister, 2013: Modeling soil moisture–precipitation feedback in the Sahel: Importance of spatial scale versus convective parameterization. *Geophys. Res. Lett.*, **40**, 6213–6218, <https://doi.org/10.1002/2013GL058511>.
- Tiedtke, M., 1989: A comprehensive mass flux scheme for cumulus parametrization in large-scale models. *Mon. Wea. Rev.*, **117**, 1779–1800, [https://doi.org/10.1175/1520-0493\(1989\)117<1779:ACMFSF>2.0.CO;2](https://doi.org/10.1175/1520-0493(1989)117<1779:ACMFSF>2.0.CO;2).
- Tuttle, S., and G. Salvucci, 2016: Empirical evidence of contrasting soil moisture–precipitation feedbacks across the United States. *Science*, **352**, 825–828, <https://doi.org/10.1126/science.aaa7185>.
- van den Hurk, B., F. Doblas-Reyes, G. Balsamo, R. D. Koster, S. I. Seneviratne, and H. Camargo, 2012: Soil moisture effects on seasonal temperature and precipitation forecast scores in Europe. *Climate Dyn.*, **38**, 349–362, <https://doi.org/10.1007/s00382-010-0956-2>.
- Wicker, L., and W. Skamarock, 2002: Time-splitting methods for elastic models using forward time schemes. *Mon. Wea. Rev.*, **130**, 2088–2097, [https://doi.org/10.1175/1520-0493\(2002\)130<2088:TSMFEM>2.0.CO;2](https://doi.org/10.1175/1520-0493(2002)130<2088:TSMFEM>2.0.CO;2).